# Lipid droplets are functionally connected to the endoplasmic reticulum in *Saccharomyces cerevisiae*

**Nicolas Jacquier[1,*], Vineet Choudhary[1,*], Muriel Mari[2], Alexandre Toulmay[1,‡], Fulvio Reggiori[2] and Roger Schneiter[1,§]**

[1]Department of Biology, Division of Biochemistry, University of Fribourg, 1700 Fribourg, Switzerland
[2]Department of Cell Biology and Institute of Biomembranes, University Medical Centre Utrecht, Heidelberglaan 3584 CX Utrecht, The Netherlands
*These authors contributed equally to this work
‡Present address: Laboratory of Cell Biochemistry and Biology, National Institute of Diabetes and Digestive and Kidney Diseases, National Institutes of Health, US Department of Health and Human Services, Bethesda, MD 20892, USA
§Author for correspondence (roger.schneiter@unifr.ch)

*Accepted 24 March 2011*
*Journal of Cell Science 124, 2424-2437*

*doi:10.1242/jcs.076836*

## Summary

Cells store metabolic energy in the form of neutral lipids that are deposited within lipid droplets (LDs). In this study, we examine the biogenesis of LDs and the transport of integral membrane proteins from the endoplasmic reticulum (ER) to newly formed LDs. In cells that lack LDs, otherwise LD-localized membrane proteins are homogenously distributed in the ER membrane. Under these conditions, transcriptional induction of a diacylglycerol acyltransferase that catalyzes the formation of the storage lipid triacylglycerol (TAG), Lro1, is sufficient to drive LD formation. Newly formed LDs originate from the ER membrane where they become decorated by marker proteins. Induction of LDs by expression of the second TAG-synthesizing integral membrane protein, Dga1, reveals that Dga1 itself moves from the ER membrane to concentrate on LDs. Photobleaching experiments (FRAP) indicate that relocation of membrane proteins from the ER to LDs is independent of temperature and energy, and thus not mediated by classical vesicular transport routes. LD-localized membrane proteins are homogenously distributed at the perimeter of LDs, they are free to move over the LD surface and can even relocate back into the ER, indicating that they are not restricted to specialized sites on LDs. These observations indicate that LDs are functionally connected to the ER membrane and that this connection allows the efficient partitioning of membrane proteins between the two compartments.

**Key words:** Endoplasmic reticulum, Lipid droplets, Organelle biogenesis, Protein transport, *Saccharomyces cerevisiae*, Triacylglycerol

## Introduction

The degradation of fatty acids through β-oxidation provides a major energy source to tissues such as liver, heart and skeletal muscle. These energy-rich fatty acids are stored in the form of neutral lipids, TAG and steryl esters (STE), within a dedicated intracellular compartment termed the lipid droplet (LD). Understanding the biogenesis of LDs during lipogenesis and their function in lipolysis is crucial to the etiology of lipid storage diseases, including type 2 diabetes (Ducharme and Bickel, 2008).

The basic structure of LDs is conserved in all eukaryotic cells. They contain a core of neutral lipids that is surrounded by a monolayer of phospholipids and a limited number of associated proteins (for reviews, see Fujimoto et al., 2008; Olofsson et al., 2009). The fact that LDs can be isolated to high purity has allowed the determination of associated proteins under various experimental conditions and in a range of cell types and organisms. Such proteomic studies have yielded inventories of LD-associated proteins that are indicative of possible interactions of LDs with other organelles, and also suggest a possible function of LDs as storage organelles for selected proteins, or as traps for unfolded or aggregated proteins (for a review, see Welte, 2007).

LDs are generally believed to form from discrete regions of the ER, where neutral lipids are synthesized, and they then aggregate within the hydrophobic core of the ER membrane. Upon reaching a critical size, LDs are then thought to bud from the ER to form an independent organelle, surrounded by a membrane monolayer that is derived from the cytoplasmic leaflet of the ER membrane. Even though this is a frequently postulated model for LD biogenesis, actual data supporting this model are rare, and alternative mechanisms for the biogenesis of LDs have also been proposed (for reviews, see Fujimoto et al., 2008; Kalantari et al., 2010; Murphy and Vance, 1999; Ploegh, 2007; Robenek et al., 2009; Waltermann et al., 2005).

LDs in yeast serve the same function and are structurally related to those of mammalian cells and plants (Leber et al., 1994). Synthesis of neutral lipids and thus LD biogenesis in yeast is under the control of four enzymes, two of which produce TAG and two make STE (Czabany et al., 2007). The acyl-CoA:sterol acyltransferases, Are1 and Are2, are polytopic ER membrane proteins that synthesize STE, whereas both Lro1 and Dga1 produce TAG. *LRO1* encodes a lecithin cholesterol acyltransferase (LCAT)-related protein that synthesizes TAG through transesterification of a fatty acid from phospholipids to diacylglycerol, whereas Dga1 catalyzes the acyl-CoA-dependent synthesis of TAG from diacylglycerol (Dahlqvist et al., 2000; Oelkers et al., 2000; Oelkers et al., 2002; Sorger and Daum, 2002). Neutral lipid synthesis and storage are dispensable for the viability of *Saccharomyces cerevisiae* because a quadruple mutant lacking all four biosynthetic enzymes is viable, makes no storage lipids and lacks detectable LDs (Oelkers et al., 2002; Sandager et al., 2002).

Targeting of proteins to LDs appears to be conserved across species because proteins associated with LDs in plant cells, for example, retain their LD localization when expressed in mammalian cells, yeast, or bacteria (Hanisch et al., 2006; Kurat et al., 2006;

Ting et al., 1997; Zehmer et al., 2008). However, how these proteins become localized to LDs is less well understood. LD-localized proteins do not contain conserved targeting sequences, but many of them contain hydrophobic sequences that harbor targeting information, because deletion of such sequences abolishes the localization of the truncated proteins to the LD and their addition to reporters is frequently sufficient for targeting to LDs (Abell et al., 2004; Hope et al., 2002; Ingelmo-Torres et al., 2009; Mullner et al., 2004; Ostermeyer et al., 2001; Subramanian et al., 2004; Zehmer et al., 2008).

In this study we use yeast strains in which the de novo formation of LDs is induced through the expression of enzymes that catalyze formation of TAG. This inducible system allowed us to monitor the biogenesis of LDs and the transport of membrane-bound LD-marker proteins from the ER membrane to the newly made LDs. The results obtained indicate that LDs are formed at the ER membrane where they rapidly become decorated with LD marker proteins. Photobleaching experiments indicate that newly synthesized membrane proteins reach LDs through a temperature- and energy-independent process and that these membrane proteins are free to move over the LD surface. The exchange of membrane proteins between the ER membrane and LDs is bidirectional, as indicated by the observation that lipolysis induces the back transport of LD-localized membrane proteins to the ER membrane, and the fact that constant photobleaching of the ER membrane reduces fluorescence of LD-localized proteins. Collectively, these data indicate that LDs do not constitute an independent cytosolic organelle, but that they are functionally connected to the ER membrane, possibly through a membrane bridge that allows the lateral partitioning of membrane proteins and possibly lipids between the two compartments through a temperature- and energy-independent, probably diffusion-driven mechanism.

## Results

We have previously identified a family of lipases that catalyze degradation of steryl esters. Two of these lipases, Tgl1 and Yeh1, localize to LDs, have predicted transmembrane domains, and biochemically behave as integral membrane proteins (Koffel et al., 2005). We wondered, therefore, how membrane proteins that are first integrated into the ER through translocon-mediated membrane insertion would reach LDs. We thus decided to investigate the targeting of membrane proteins from the ER to LDs in more detail.

Therefore, we first examined the fate of LD-localized integral membrane proteins in yeast cells that have no STE (*are1Δ are2Δ*), no TAG (*dga1Δ lro1Δ*) or no neutral lipids at all and hence no LDs (*dga1Δ lro1Δ are1Δ are2Δ*). Lack of STE or TAG alone did not affect LD formation as visualized by Nile Red staining, a lipophilic dye that specifically stains LDs, and did not affect LD targeting of GFP-tagged Erg6, a Δ24 sterol methyltransferase required for the synthesis of the fungal ergosterol, and an established LD marker protein (Leber et al., 1994) (Fig. 1A). Erg6–GFP was solubilized only upon detergent treatment of membranes, and hence biochemically behaves as an integral membrane protein even though the protein has no predicted transmembrane domains (supplementary material Fig. S1). In the absence of LDs, however, Erg6–GFP was localized to the nuclear and peripheral ER, as indicated by the circular staining pattern and by its colocalization with the ER luminal marker protein, Kar2–mRFP–HDEL (Gao et al., 2005) (Fig. 1A,B). ER localization in the absence of neutral lipids was not only observed for Erg6 but also for Tgl1 and Yeh1, and thus is a more general property of LD-localized membrane proteins (Fig. 1B). The fact that LD-localized membrane proteins were confined to the ER in cells that had no neutral lipids indicates that these proteins are probably first inserted into the ER membrane, from where they are transported to LDs, or, that their localization to LDs occurs during biogenesis of LDs themselves and thus may reflect the biogenetic origin of LDs from the ER membrane.

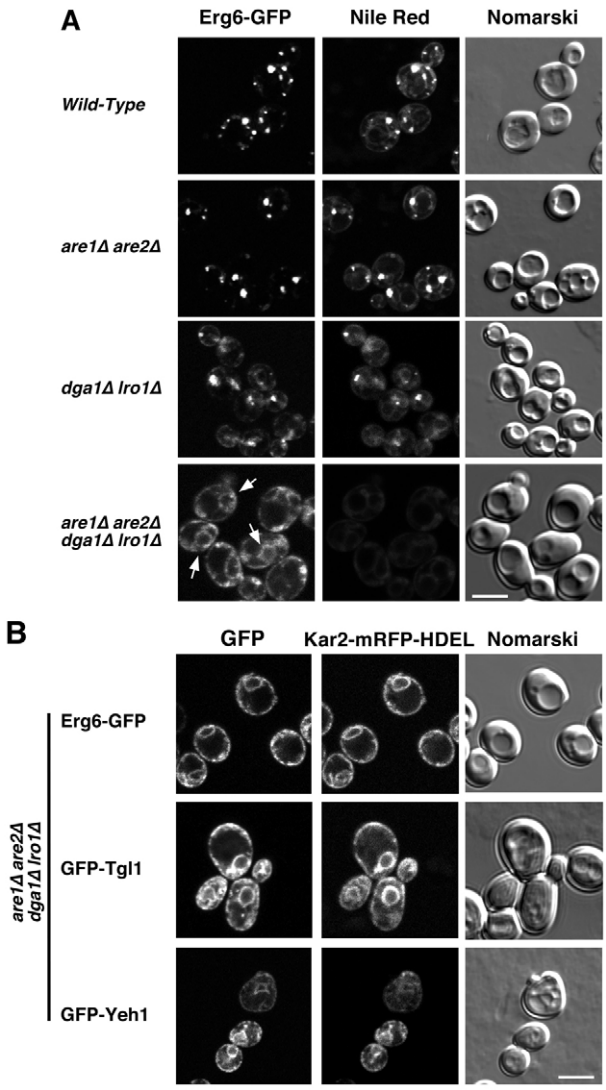


**Fig. 1. Localization of LD proteins to the ER in the absence of neutral lipids.** (**A**) LDs in strains of the indicated genotypes that express the LD marker protein Erg6–GFP were stained with Nile Red and the colocalization of LDs with Erg6–GFP was examined by confocal microscopy. ER localization of Erg6–GFP in the quadruple mutant that lacks neutral lipids is indicated by arrows. (**B**) LD proteins (Erg6–GFP, GFP–Tgl1 or GFP–Yeh1) colocalize with the ER marker Kar2–mRFP–HDEL in the absence of neutral lipids in the quadruple mutant cells. Scale bars: 5 μm.

### Induction of neutral lipid formation results in LD formation at the ER membrane

To examine the fate of ER-localized LD-marker proteins during the biogenesis of LDs, we generated strains in which the transcription of genes for enzymes that catalyze the synthesis of TAG could be induced by a switch in carbon source. Because strains that express only one of the four neutral lipid biosynthetic

genes have LDs, induction of TAG synthesis is expected to induce de novo formation of LDs (Sandager et al., 2002). Yeast has two enzymes that catalyze TAG formation, Lro1 and Dga1. Because Lro1 is an ER localized enzyme with one predicted transmembrane domain, we first examined LD formation and the fate of LD-localized membrane proteins upon induction of Lro1 (see http://organelledb.lsi.umich.edu) (Dahlqvist et al., 2000; Oelkers et al., 2000). Therefore, expression of *LRO1* was placed under the control of a galactose-inducible promoter. Induction of *GAL–LRO1* expression in a genetic background in which the other three genes for neutral lipid synthesis were deleted (*dga1Δ are1Δ are2Δ*) resulted in the rapid appearance of TAG, as monitored by radiolabeling of newly synthesized lipids with [$^3$H]palmitate. In the presence of glucose, i.e. without induction of Lro1, no formation of TAG was observed, indicating tight repression of *GAL-LRO1* expression (Fig. 2A,B).

Next, we examined the localization of the lipid droplet marker protein Erg6–RFP during induction of TAG formation. Without induction, Erg6–RFP uniformly labeled the ER membrane and no LDs were detectable by staining with the lipophilic fluorescent dye BODIPY 493/503, which specifically stains LDs, thus confirming that LD-localized proteins are present in the ER in cells that have no LDs (Gocze and Freeman, 1994) (Fig. 2C, arrow). Within 30 minutes of Lro1 expression, however, Erg6–RFP lost its uniform ER localization and was found instead to have a punctate localization pattern (Fig. 2C, 30 minutes, arrowheads). The punctate structures that were decorated by Erg6–RFP appeared to localize to or adjacent to the ER membrane, which remained faintly stained in these cells. The punctate structures marked by Erg6–RFP also appeared to contain TAG because they colocalized with BODIPY-stained structures. The colocalization of the LD-marker protein Erg6–RFP and BODIPY in punctate structures that localize in or adjacent to the ER membrane indicates that these structures represent early stages of LD formation. After 2 hours of *LRO1* induction, the number of punctate structures increased to resemble that of LDs in wild-type cells (Fig. 2C, 120 minutes). Relocation of Erg6–RFP from an uniform ER distribution to a punctate distribution was also observed when protein synthesis was inhibited

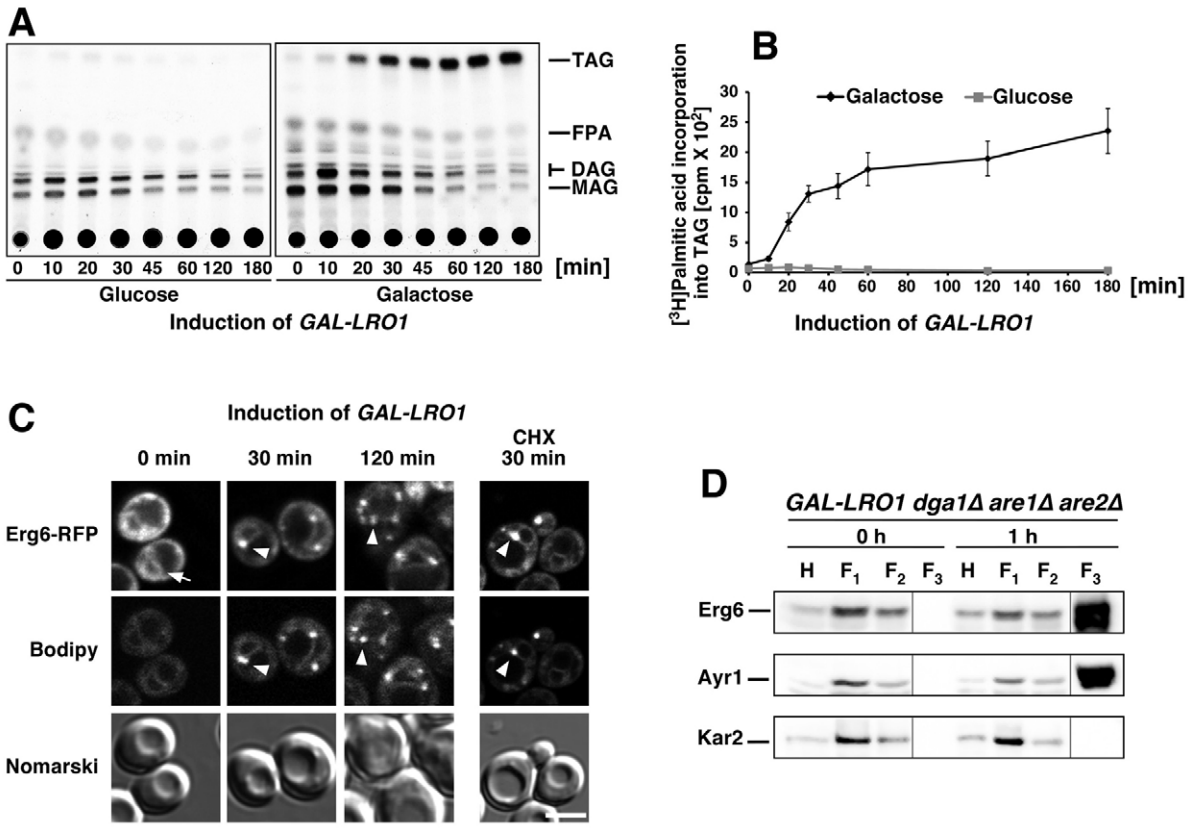


**Fig. 2. Induction of neutral lipid synthesis results in biogenesis of LDs from the ER membrane.** (**A**) Time dependence of *GAL-LRO1* induction was followed by monitoring TAG formation. Cells were cultured in raffinose-containing medium overnight, diluted and switched into medium containing either glucose or galactose. Lipids were labeled by the addition of [$^3$H]palmitate, samples were removed at the time points indicated and lipids were extracted and analyzed by TLC. The position of diacylglycerol (DAG), monoacylglycerol (MAG), free palmitic acid (FPA) and TAG is indicated. (**B**) Quantification of TAG formation upon Lro1 induction. Formation of radiolabeled TAG was quantified by radioscanning of thin-layer chromatograms as shown in A. (**C**) Induction of neutral lipid synthesis results in relocation of Erg6–RFP. Cells expressing *GAL-LRO1* and Erg6–RFP were switched from raffinose- to galactose-containing medium and the localization of Erg6–RFP relative to BODIPY-stained LDs was examined at the indicated time points by confocal microscopy. Localization of Erg6–RFP to the ER in the absence of Lro1 induction is indicated by an arrow. Colocalization of Erg6–RFP with BODIPY-stained punctate structures is indicated by arrowheads. In the panel to the right, cycloheximide (CHX; 50 μg/ml) was added 15 minutes after induction of Lro1 and cells were monitored 30 minutes after induction. Scale bar: 5 μm. (**D**) Fractionation of the LD marker proteins Erg6 and Ayr1 upon Lro1 induction. The *GAL-LRO1* strain of the indicated genotype was switched from raffinose- to galactose-containing medium and LDs were isolated by three successive flotations at 0 hours or 1 hour after the galactose shift. Samples were removed from the cell homogenate (H), each of the flotating fractions ($F_1$, $F_2$, $F_3$), and the relative enrichment of the LD marker proteins Erg6 and Ayr1 or that of the ER luminal chaperone Kar2 was analyzed by western blotting. Samples were detected with identical exposure settings. Vertical lines indicate lanes that were removed.

by cycloheximide 15 minutes after induction of Lro1 synthesis, indicating that the pre-existing pool of Erg6–RFP relocated to these punctate structures (Fig. 2C, CHX, 30 minutes). This relocation of ER membrane proteins upon induction of TAG synthesis was observed not only with Erg6 but also with Tgl1 and Yeh1 (supplementary material Fig. S2). Thus these data indicate that induction of TAG formation results in the de novo formation of LDs in the ER membrane and that ER-localized LD marker proteins concentrate over neutral lipid-containing structures in the ER.

To determine whether LD formation through the induction of *LRO1* expression altered not only the subcellular localization of the LD marker protein Erg6, but also its biochemical fractionation properties, as would be expected if the protein localized to LDs, we compared the fractionation properties of Erg6 from cells lacking LDs with those of cells induced to express Lro1 for 1 hour. LDs have a characteristic low density and they can be isolated by three consecutive flotation steps through gradients of reduced density (12% Ficoll, 8% Ficoll and 0.25 M sorbitol). This fractionation protocol results in a strong, roughly 100-fold enrichment of neutral lipids and LD-localized marker proteins in the final floating fraction ($F_3$) compared with their relative concentration in the cell homogenate (Leber et al., 1994; Schneiter et al., 1999). Without induction of *LRO1*, the two LD marker proteins Erg6 and Ayr1, a NADPH-dependent 1-acyl dihydroxyacetone phosphate reductase, were enriched in the first floating fraction (Athenstaedt and Daum, 2000) (Fig. 2D, $F_1$). The same $F_1$ was also enriched in the ER luminal chaperone Kar2, indicating that Erg6 and Ayr1 are enriched in an ER fraction in cells that have no LDs, as was observed before by differential centrifugation (Sorger et al., 2004). However, when cells were fractionated after induction of *LRO1* expression for 1 hour, Erg6 and Ayr1 were strongly enriched in the $F_3$ (Fig. 2D, 1 hour, $F_3$). This enrichment of Erg6 and Ayr1 in $F_3$ was not observed when the floating fraction was isolated from cells lacking LDs (Fig. 2D, 0 hours, $F_3$). These biochemical data thus indicate that induction of *LRO1* expression results in the enrichment of LD marker proteins in a low-density fraction. Because LDs from wild-type cells are also enriched in $F_3$, we conclude that induction of *LRO1* expression results in the formation of structures with the same fractionation properties as is characteristic for LDs of wild-type cells.

### The TAG biosynthetic integral membrane protein Dga1 relocates from the ER to LDs

Dga1 catalyzes TAG formation through the acyl-CoA-dependent acylation of diacylglycerol (DAG) and its activity is present both in microsomes and isolated LDs (Oelkers et al., 2002; Sorger and Daum, 2002). To examine this dual localization of Dga1 during LD biogenesis, we placed expression of an N-terminally GFP-tagged version of Dga1 under the control of a galactose-inducible promoter. Expression of GFP–Dga1 in a triple mutant background (*lro1Δ are1Δ are2Δ*) resulted in the time-dependent formation of TAG as revealed by labeling with [$^3$H]palmitic acid (supplementary material Fig. S3). Colocalization of GFP–Dga1 and Erg6–RFP during LD formation revealed that GFP–Dga1 was localized to the ER for up to 6 hours during induction. LDs, however, appeared after just 2 hours of induction, as indicated by the punctate localization of Erg6–RFP (Fig. 3A). After 8 hours of Dga1 induction, however, GFP–Dga1 labeled punctate structures that overlapped with those marked by Erg6–RFP, indicating that the protein had relocated from the ER to LDs (Fig. 3A, 8 hours,

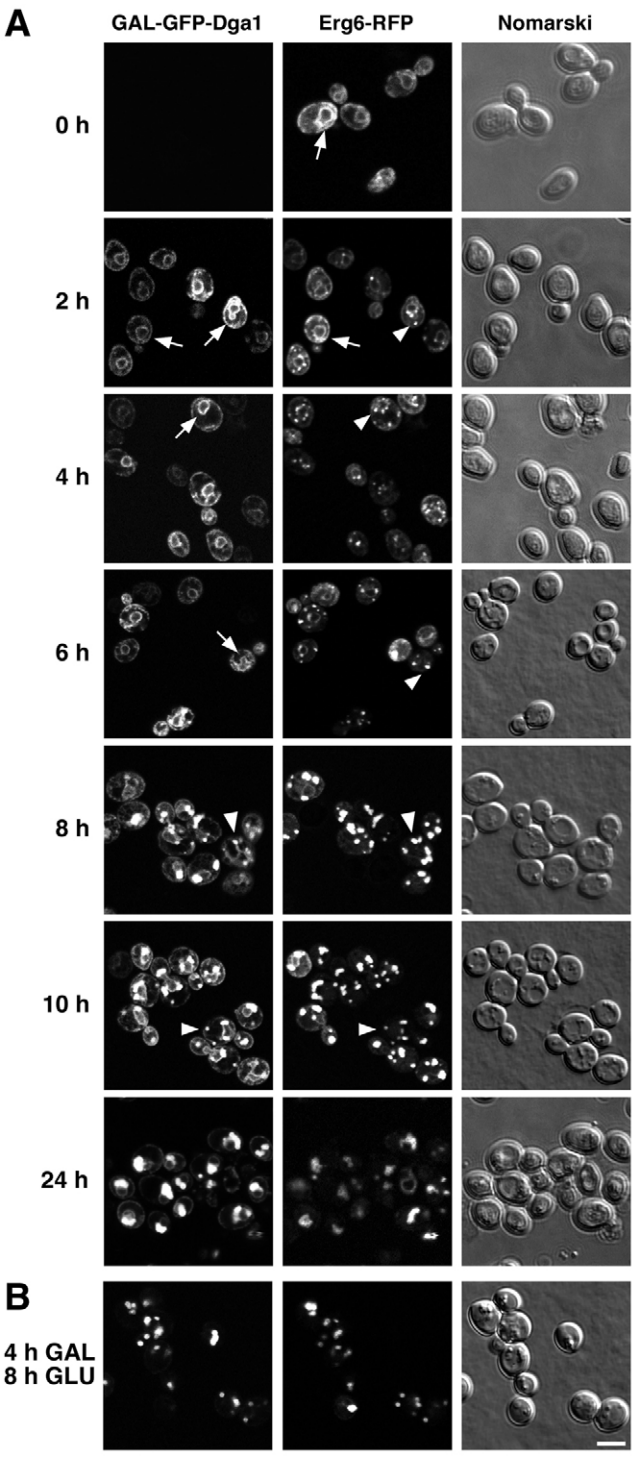


**Fig. 3. Relocation of Dga1 from the ER to LDs.** (**A**) Cells expressing *GAL–GFP–Dga1* and Erg6–RFP in a *lro1Δ are1Δ are2Δ* mutant background were cultured in raffinose-containing medium and switched to galactose-containing medium (GAL) for the periods of time indicated, and the localization of GFP–Dga1 and Erg6–RFP was analyzed by confocal microscopy. Arrows indicate the ER (circular), arrowheads indicate LDs (punctate). (**B**) Relocation of GFP–Dga1 does not depend on its ongoing synthesis. Expression of GFP–Dga1 was induced for 4 hours, cells were shifted to glucose-containing medium (GLU) for 8 hours, and the distributions of GFP–Dga1 and Erg6–RFP were monitored by confocal microscopy. Scale bar: 5 μm.

arrowheads). Upon longer times of induction the punctate structures increased in size and GFP–Dga1 completely colocalized with Erg6–RFP after 24 hours of induction (Fig. 3A, 24 hours). Colocalization of Dga1 and Erg6 was also observed if Dga1 expression was first induced by galactose for 4 hours and then repressed by shifting cells to glucose-containing medium for 8 hours, indicating that the transport of Dga1 from the ER to LDs reflects movement of the pre-existing protein (Fig. 3B). Fractionation and protease protection experiments indicate that Dga1 encodes an integral membrane protein with at least two transmembrane domains and a topology similar to that of its DGAT2 orthologs from plants and mammals (Shockey et al., 2006; Stone et al., 2006) (supplementary material Fig. S4). Because integral membrane proteins insert into the ER membrane by translocon-mediated integration of their transmembrane domains, relocation of Dga1 from the ER to LDs is likely to take place through a pathway that maintains its membrane insertion.

Analysis of the time-dependent relocation of Dga1 from the ER to LDs at the ultrastructural level by immunoelectron microscopy [IEM; using a cryosectioning protocol adapted from the method of Tokuyasu (Tokuyasu, 1973)] revealed that immunogold-labeling of GFP–Dga1 decorated the ER membrane in cells that were induced to express the protein for 4 hours (Griffith et al., 2008) (Fig. 4C,D). The labeling was highly specific as no background staining was observed in cells that were cultured without induction of GFP–Dga1 (Fig. 4A,B). After 8–24 hours of GFP–Dga1 induction, gold particles specifically stained the periphery of electron-translucent LDs (Fig. 4E–H). The number and surface area of LDs increased in a time-dependent manner during Dga1 induction (Fig. 5A,C). The surface area of the ER, by contrast, remained constant (Fig. 5C). However, gold particles were redistributed from the ER membrane to the LDs, whereas the low background labeling of mitochondria remained constant (Fig. 5B,D). These data thus strongly support the notion that induction of Dga1 results in a time-dependent induction of LD biogenesis and that Dga1 itself shows a time-dependent relocation from its initial localization in the ER membrane to LDs. The observation that the gold particles decorate the periphery of the LDs indicates that Dga1 not only concentrates at sites of contact between the ER and LDs but that it decorates the entire perimeter of LDs as well.

### Relocation of Dga1 to LDs is independent of energy

To examine the relocation of Dga1 from the ER to LDs in more detail, we first determined whether the late relocation of Dga1 observed upon LD formation is also observed if GFP–Dga1 expression is induced in cells that contain pre-existing LDs. Expression of GFP–Dga1 in wild-type cells revealed that Dga1 was first homogenously localized in the ER, whereas Erg6–RFP stained the pre-existing LDs (Fig. 6A). Only after 6 hours of induction did GFP–Dga1 begin to label punctate structures that overlapped with Erg6–RFP. These data, therefore, indicate that the initial localization of GFP–Dga1 to the ER is also observed if cells contain pre-existing LDs as a result of the activities of the neutral lipid biosynthetic enzymes Lro1, Are1 and Are2. Thus, relocation of Dga1 to LDs does not depend on LD formation through Dga1-dependent induction of TAG synthesis and so is independent of the time when LDs are formed. Relocation of Dga1 to LDs was also observed when GFP–Dga1 expression was repressed by shifting cells to glucose-containing medium after 4 hours of induction, indicating that relocation is the result of transport of the pre-existing protein (Fig. 6B).

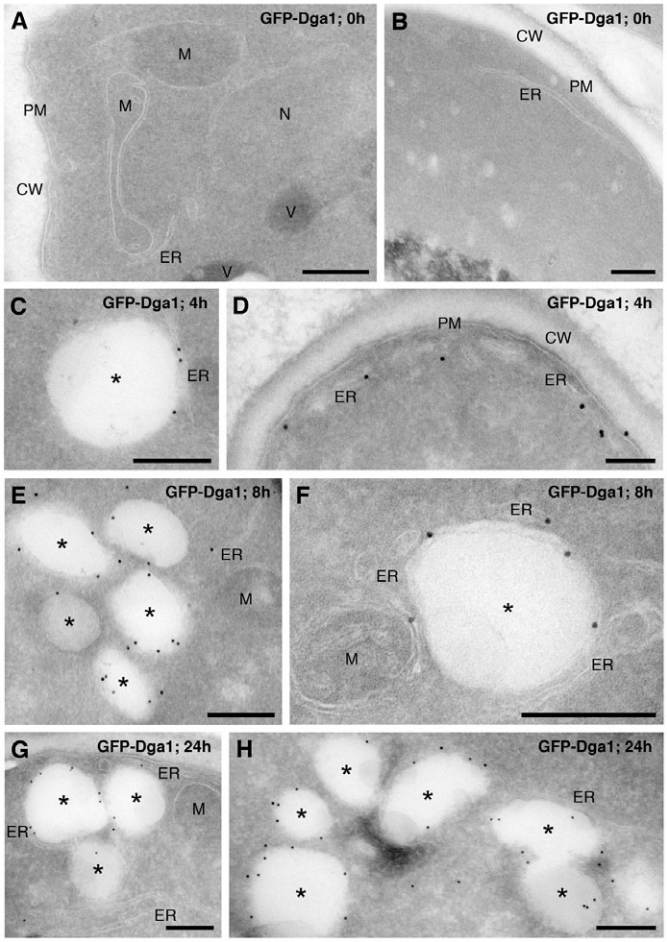


**Fig. 4. IEM to detect the location of GFP–Dga1 at different time points during induction.** Cells expressing *GAL–GFP–DGA1* in a *lro1Δ are1Δ are2Δ* mutant background were cultured in raffinose-containing medium and switched to galactose-containing medium for the periods of time indicated, and the location of GFP–Dga1 analyzed by IEM. Cells were collected after 0 hours (**A**,**B**), 4 hours (**C**,**D**), 8 hours (**E**,**F**) and 24 hours (**G**,**H**) of induction and processed for IEM as described in the Materials and Methods. Cryosections were immunogold labeled to detect the GFP–Dga1 fusion protein. CW, cell wall; ER, endoplasmic reticulum; M, mitochondrion; N, nucleus; PM, plasma membrane; V, vacuole. LDs are marked with asterisks. Scale bars: 200 nm.

To examine the mechanism of the protein transport pathway that results in relocation of Dga1 to LDs in more detail, we performed photobleaching experiments (fluorescence recovery after photobleaching; FRAP). Cells expressing GFP–Dga1 were cultured in galactose-containing medium for 6–8 hours, and individual LDs were then photobleached and recovery of fluorescence over time was recorded. These experiments revealed that LD-localized GFP–Dga1 recovered from photobleaching to approximately 66.1±6.0% of the initial fluorescence over a time period of 300 seconds, indicating that a sizable non-bleached pool of GFP–Dga1 is free to exchange with the photobleached pool that is localized on LDs (Fig. 6C). Quantitative analysis of the FRAP results, assuming diffusion of GFP–Dga1 within the plane of a membrane, revealed that the LD-localized Dga1 recovered from photobleaching with a mobile fraction ($M_f$) of 85% and a half-life ($t_{1/2}$) of 82.9 seconds (Ellenberg et al., 1997; Lippincott-Schwartz et al., 2001). When

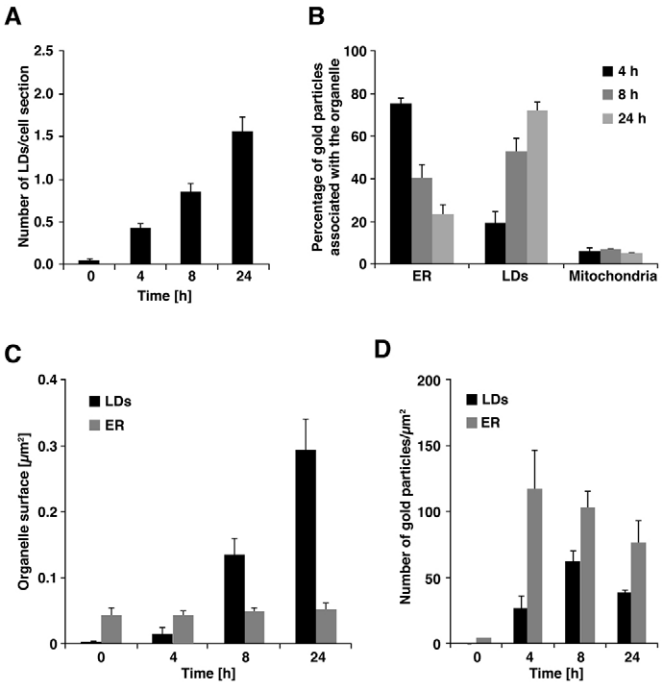


**Fig. 5. Quantitative analyses of the relocation of Dga1 from the ER to LDs as observed by immunogold labeling.** (**A**) Time-dependent increase in the number of LDs upon induction of Dga1. The number of LDs per cell section at each time point was determined in 100 randomly selected cell profiles. (**B**) Relocation of GFP–Dga1 over time. The relative abundance of gold particles on the ER, LDs and mitochondria was determined by counting particles in the vicinity (≤25 nm) of the organelle of interest. Mitochondria were selected to estimate the labeling background. (**C**) The surface area of LDs increases over time. The organelle surface area was measured as described in the Materials and Methods. (**D**) Density of gold label over the ER and LDs. Labeling density was determined by linear density measurement. All the differences are statistically significant ($P$<0.05).

the mobility of Dga1 was analyzed after 4 hours of induction, i.e. when the protein was still homogenously distributed within the ER membrane, it had an $M_f$ of 97% and recovered from photobleaching with a $t_{1/2}$ of 14.7 seconds. These results indicate that relocation of the protein to LDs results in a slight decrease in its $M_f$ but in a substantial increase of its $t_{1/2}$, suggesting that the mobility of LD-localized Dga1 is reduced compared with that in the ER membrane. This reduced mobility of the LD-localized protein might be explained by the unusual structure and/or composition of the limiting membrane of LDs or by its transient interaction with a confined substrate, such as LD-localized DAG. FRAP measurements of free GFP ($M_f$=97%, $t_{1/2}$=0.3 seconds), an ER membrane protein (Sec63–GFP; $M_f$=70%, $t_{1/2}$=8.3 seconds), a plasma membrane protein (Pma1–GFP; $M_f$=40%, $t_{1/2}$=165.8 seconds) and of an immobile chromatin component (Hhf1–GFP; $M_f$=8%) indicate that our FRAP measurements monitored the relative mobility of these different proteins (Malinska et al., 2004; Nikonov et al., 2002; van Drogen et al., 2001) (supplementary material Fig. S5A). Fluorescence recovery of GFP–Dga1 cannot be explained by refolding of the fluorophore after photobleaching because there is no significant recovery of fluorescence after photobleaching of whole cells (supplementary material Fig. S5B). The observed recovery of LD-localized GFP–Dga1 thus indicates that the bleached pool of the protein that is localized on LDs can rapidly exchange with a non-bleached pool of Dga1, possibly via the ER membrane or through adjacent LDs.

To examine whether synthesis of new proteins was required to replace the photobleached pool of GFP–Dga1 on LDs, translation was blocked by treating cells with cycloheximide. FRAP analysis of cells that were incubated with this drug for 15 minutes before FRAP found that GFP–Dga1 recovered with a $M_f$ of 60% and a $t_{1/2}$ of 26.5 seconds, indicating that the exchange of LD-localized Dga1 was independent of ongoing translations (Fig. 6D, CHX). Moreover, pre-incubating the cells on ice or depleting ATP levels, by the addition of azide and fluoride, did not significantly decrease the $M_f$ or the $t_{1/2}$ of fluorescence recovery of the LD-localized protein (Fig. 6D). However, under the conditions used here to monitor FRAP of LD-localized GFP–Dga1, the temperature- and energy-dependent uptake of the endocytosed fluorescent dye FM4-64 was arrested, indicating that the temperature- and energy-depletion treatments were effective (Vida and Emr, 1995) (supplementary material Fig. S6). These results thus indicate that a pre-existing pool of the membrane protein GFP–Dga1 can move onto LDs by an energy- and temperature-independent mechanism. Because vesicle formation and fusion are energy dependent and sensitive to low temperature, these results suggest that transport of membrane proteins from the ER to LDs is independent of classical vesicular transport routes. Consistent with this notion, mutations that conditionally block formation of COPII-coated vesicles (*sec12*), vesicle fusion (*sec18*) or formation of COPI-coated vesicles (*sec21* and *sec27*) did not significantly delay fluorescence recovery of LD-localized GFP–Dga1 upon photobleaching (supplementary material Fig. S7A,C). Maturation of a secretory cargo protein, carboxypeptidase Y, however, was either completely blocked or strongly delayed in these mutants (supplementary material Fig. S7B,D).

FRAP experiments with another LD-localized membrane-bound protein, GFP–Erg6, revealed that it also recovered from photobleaching, albeit with a slightly lower $M_f$ than Dga1 ($M_f$=60%, $t_{1/2}$=132.6 seconds). Similar to that observed for GFP–Dga1, fluorescence recovery of GFP–Erg6 was independent of ongoing translation and was also temperature- and energy-independent (supplementary material Fig. S8). These data suggest that LD-localized membrane proteins might generally be free to move onto LDs and that the transport of these proteins relies on a mechanism that is independent of energy and temperature. The temperature- and energy-independence of the protein transport mechanism together with the fact that the observed rate of fluorescence recovery of Dga1 and Erg6 is characteristic for a two-dimensional diffusion of membrane proteins, suggest that LD localization could occur by lateral diffusion of the proteins within a continuous membrane system (Ellenberg et al., 1997; Lippincott-Schwartz et al., 2001).

### LD-localized membrane proteins encircle the neutral lipid core and freely move over the LD surface

The rapid recovery of LD-localized membrane proteins observed by FRAP suggests that LDs stay functionally connected to the ER membrane and that the transport of membrane proteins from the ER to LDs might occur through this connection. Morphological analyses indicate that the ER is frequently in close association with LDs and that the ER membrane follows the curvature of the LD surface over some distance (Fig. 4C; Fig. 7A). However, the precise arrangement between the ER membrane bilayer and the

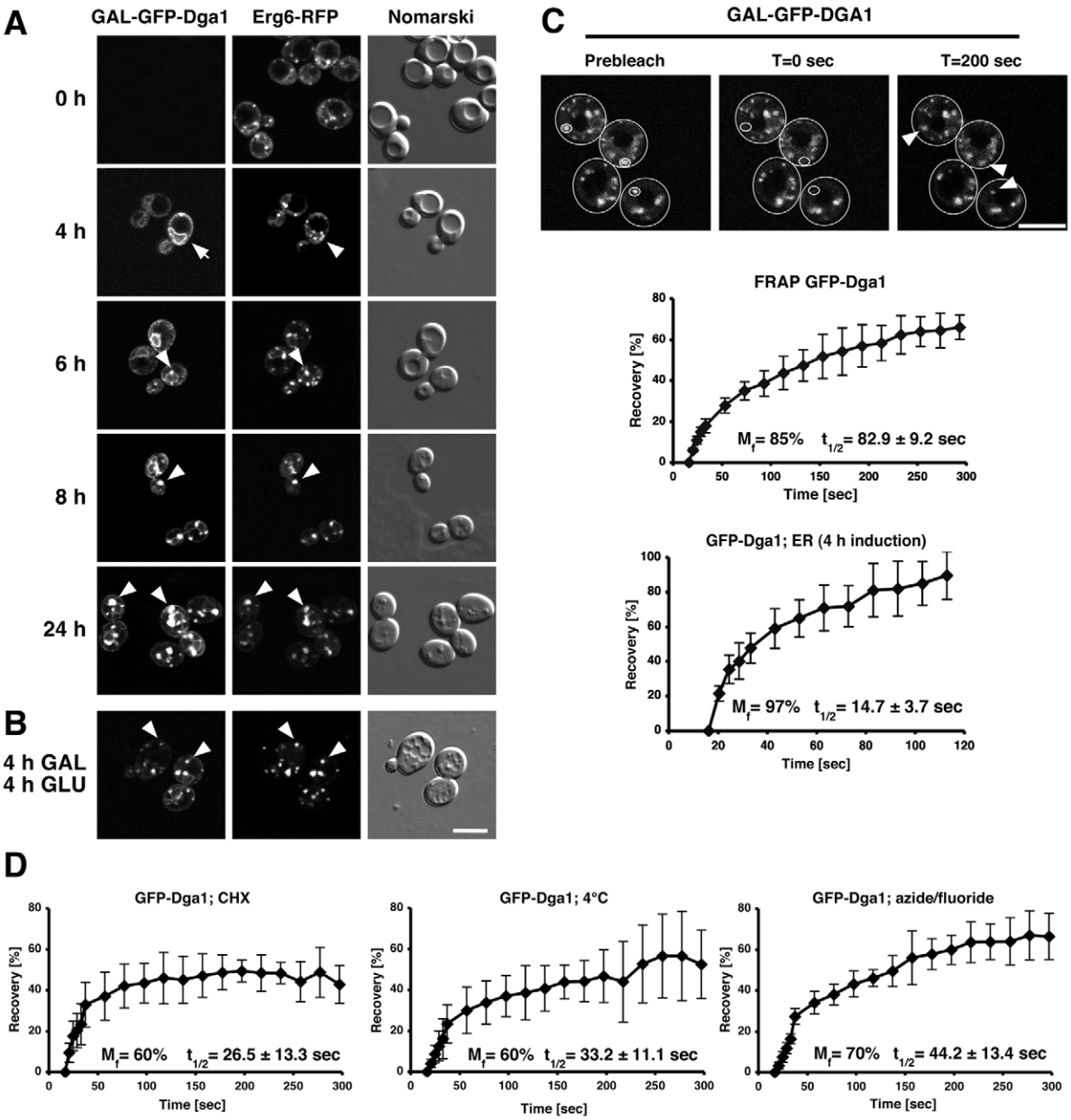


**Fig. 6. Relocation of Dga1 to LDs is energy independent.** (**A**) GFP–Dga1 moves from the ER to LDs in wild-type cells. Wild-type cells expressing GAL–GFP–Dga1 and Erg6–RFP were shifted to galactose-containing medium for the times indicated and analyzed by confocal microscopy. The arrow indicates the ER (circular), arrowheads indicate LDs (punctate). (**B**) Relocation of GFP–Dga1 from the ER to LDs is independent of continued synthesis of GFP–Dga1. Cells were incubated for 4 hours in galactose-containing medium (GAL) to induce expression of GFP–Dga1 and then shifted to glucose-containing medium (GLU) to repress expression of the marker protein. (**C**) Photobleaching reveals exchange of LD-localized GFP–Dga1. Cells were cultured in galactose-containing medium for 6–8 hours, individual LDs (circled) were photobleached at 0 seconds, and recovery of fluorescence was monitored over time. The perimeter of the cells is indicated by oval lines. LDs that were photobleached are indicated by arrowheads and fluorescence recovery is shown 200 seconds after photobleaching. The time-dependent recovery of fluorescence is shown in the graph (values are means ± s.d., *n*=9 LDs). FRAP analysis of ER-localized GFP–Dga1 from cells induced for 4 hours is shown for comparison. (**D**) Exchange of GFP–Dga1 on LDs is energy independent. GFP–Dga1 was induced, cells were treated with cycloheximide (CHX, 50 µg/ml), placed on ice (4°C), or treated with $NaN_3$ and NaF (20 mM each) prior to photobleaching and recording of fluorescence recovery (values are means ± s.d.; *n*=9 LDs for each experiment). Scale bars: 5 µm.

possible monolayer surrounding the LD cannot unambiguously be resolved even by conventional electron microscopy.

Because the ER in these electron micrographs only partially follows the LD contour rather than encircling the core of the LD completely, we wondered whether the LD-localized membrane proteins would localize only at sites where the ER membrane contacts the LD or whether these proteins would homogenously distribute over the entire spherical periphery of the LD. To this end, cells expressing GFP–Dga1 from the galactose-inducible promoter were cultured overnight in galactose-containing medium to induce formation of large LDs. Confocal microscopy of GFP–Dga1 and Erg6–RFP localization in cells with large LDs revealed

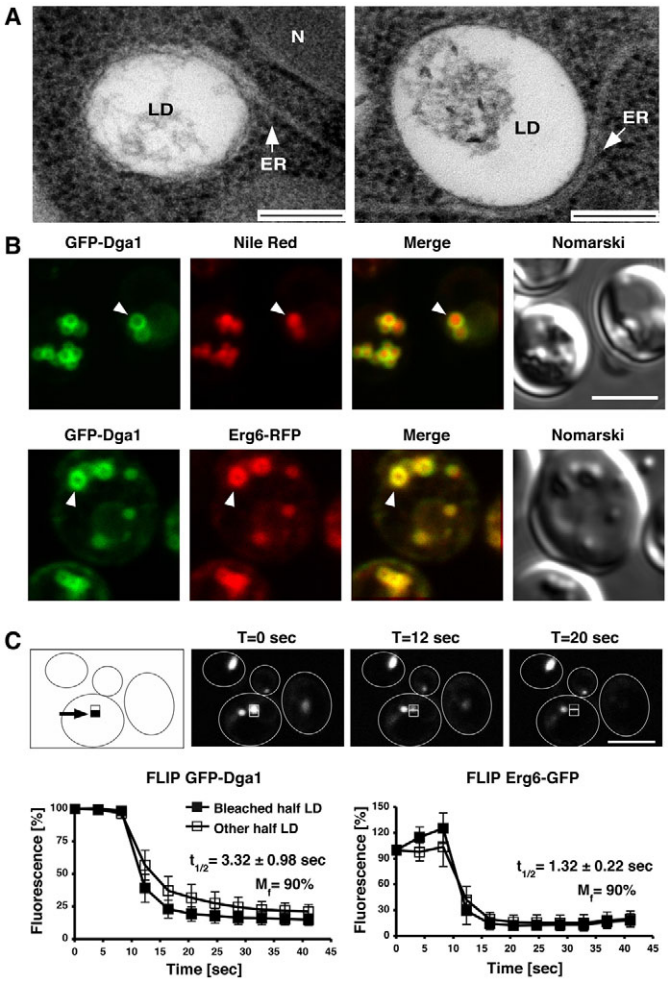


**Fig. 7. Dga1 surrounds LDs and is free to move over the LD surface.** (**A**) The ER membrane closely associates with LDs. Wild-type cells were high-pressure frozen and analyzed by EM. The ER membrane is indicated by arrows. N, nucleus. Scale bars: 0.2 µm. (**B**) LD-localized membrane proteins surround the neutral lipid core. Cells expressing GAL–GFP–Dga1 were cultured in galactose-containing medium overnight to induce the formation of large LDs, stained with Nile Red and analyzed by confocal microscopy. The lower panels show colocalization of GFP–Dga1 with Erg6–RFP within a circular structure (arrowheads). Scale bar: 5 µm. (**C**) LD-localized membrane proteins are mobile over the LD surface. Cells expressing GFP-tagged Dga1 or Erg6 were analyzed by confocal microscopy. Half of an LD was constantly photobleached (black box) and time-dependent fluorescence loss in the other half of the LD was monitored (open box). Time-dependent loss of fluorescence in the photobleached and non-bleached part of the LD is plotted in the graphs (values are means ± s.d.; $n$=9). Scale bar: 5 µm.

that GFP–Dga1 stained a circular structure that surrounded the neutral lipid core, which was stained by Nile Red. GFP–Dga1 and Erg6–RFP colocalized in these circular structures (Fig. 7B). These data are thus consistent with the observed gold labeling at the perimeter of LDs, seen by IEM, and indicate that LD-localized membrane proteins are not concentrated at a distinct interface between the ER and LDs, or at proposed sites of local bilayer formation, but that they are homogenously distributed over the entire periphery of the LD (Ploegh, 2007) (Fig. 4).

To examine whether these LD-localized proteins are free to move within their peripheral location we performed fluorescence loss in photobleaching (FLIP) experiments. Therefore, half of an LD stained by either Dga1–GFP or by Erg6–GFP was constantly photobleached and loss of fluorescence in the non-photobleached half of the LD was monitored. These experiments revealed that fluorescence in the non-photobleached part of the LD decreased as rapidly as the fluorescence in the photobleached half, indicating that these membrane proteins rapidly equilibrated over the entire surface of the LD and that they were not confined to a specific region of the LD, such as the contact sites between the LDs and the ER membrane (Fig. 7C). The observation that fluorescence loss occurred with similar rates in all the LDs analyzed, indicates that it is not due to rotation of the LD itself, which would be expected to occur at random angles with respect to the bleaching area and thus would also give rise to LDs that did not loose fluorescence upon photobleaching if they constantly exposed the site to the bleaching box.

### LD-localized membrane proteins can move back into the ER

Given that integral membrane proteins can relocate from a homogenous circular ER localization to a punctate localization on LDs, one might expect that the mobilization of neutral lipids and the concomitant regression of LDs would result in a reversal of this process. To examine whether lipolysis induces the back transport of LD-localized membrane proteins to the ER, we first induced GFP–Dga1 expression using galactose-containing medium and then shifted the cells to glucose-containing medium to repress its expression. Lipolysis was then induced by the addition of the fatty acid synthase inhibitor cerulenin. To simultaneously monitor disappearance of LDs and the subcellular localization of GFP–Dga1, cells were stained with Nile Red and analyzed by confocal microscopy. These experiments revealed that GFP–Dga1 relocated from LDs back to the ER when cells were grown in the presence of cerulenin for 2–6 hours (Fig. 8A). In the absence of cerulenin, however, GFP–Dga1 colocalized with punctate Nile-Red-stained structures, indicating that the protein remained localized to LDs. The back transport of GFP–Dga1 from LDs to the ER thus depends on lipolysis induced by cerulenin. To monitor the extent of lipolysis in the presence or absence of cerulenin, cells were labeled with [$^3$H]palmitic acid and TAG levels were determined. This analysis revealed that repression of GFP–Dga1 expression by shifting the cells to glucose-containing medium alone was not sufficient to induce lipolysis, but that the presence of cerulenin resulted in an approximately fivefold reduction of TAG levels over the 6 hours timefi period (Fig. 8B). The results of these experiments thus indicate that LD-localized membrane proteins can move from their LD location back into the ER upon lipolysis of neutral lipids and turnover of LDs.

To examine whether LD-localized membrane proteins could move from LDs into the ER bilayer membrane even without induction of lipolysis, we constantly photobleached the nuclear membrane and monitored fluorescence loss over LDs marked by GFP–Dga1. These experiments revealed the presence of two classes of LDs, which lost fluorescence at different rates upon photobleaching of the nuclear membrane. LDs in the vicinity of the nuclear membrane (proximal LDs) exhibited constant loss of fluorescence whereas LDs localized at the cell perimeter (distal LDs) were less sensitive to the photobleaching of the nuclear ER (Fig. 8C). The results of these FLIP experiments indicate that perinuclear LDs rapidly exchange their membrane proteins with the nuclear ER even under conditions of lipogenesis, suggesting constant exchange of membrane proteins between the ER and

LDs. The observation that the distal LDs do not lose fluorescence upon photobleaching of the nuclear ER could indicate that the peripheral ER might not be connected to the perinuclear ER or that the diffusion between the two ER domains is slow in comparison with the one seen between the nuclear membrane and the proximal LDs.

To examine the energy and temperature dependence of the back transport of Dga1 from the LDs to the ER membrane, cells were

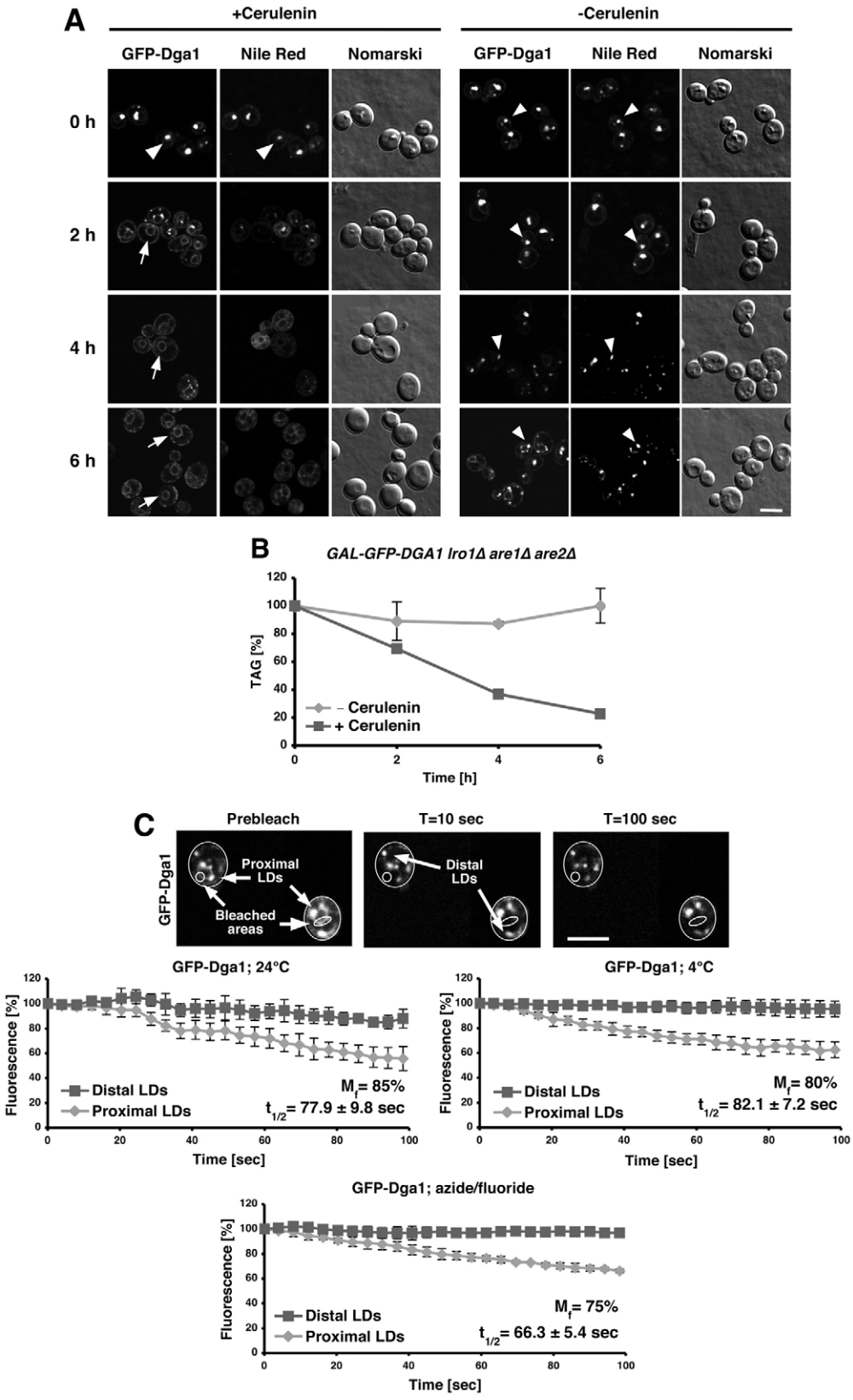


**Fig. 8. Dga1 moves from LDs back into the ER membrane.** (**A**) Lipolysis induces movement of Dga1 from LDs into the ER. Cells were cultured in galactose-containing medium to induce expression of GFP–Dga1 and shifted to glucose-containing medium lacking or containing the fatty acid synthase inhibitor cerulenin (10 μg/ml) to induce turnover of TAG. After the indicated periods of time, LDs were stained with Nile Red and cells were examined by confocal microscopy. Arrows indicate circular ER localization, arrowheads indicate punctate LD localization. Scale bar: 5 μm. (**B**) The progression of lipolysis was monitored by labeling cells with [$^3$H]palmitic acid prior to their shift into glucose-containing medium. Lipids were separated by TLC and quantified by radioscanning. (**C**) LD-localized membrane proteins equilibrate with the ER membrane. Expression of GFP–Dga1 was induced by galactose for 20 hours, cells were analyzed by confocal microscopy and a region of the nuclear membrane was constantly photobleached. Time-dependent loss of fluorescence was monitored in LDs that were close to the nuclear membrane (proximal LDs) or in LDs that were located at the periphery of the cells (distal LDs; values are means ± s.d.; *n*=9). To determine the energy and temperature dependence of the back transport, cells were treated with $NaN_3$ and NaF (20 mM each), or placed on ice (4°C), before photobleaching. Scale bar: 5 μm.

treated with sodium azide and sodium fluoride or chilled on ice before photobleaching of the nuclear ER. Under these conditions, fluorescence of the perinuclear LDs decreased at rates that are comparable with the loss of fluorescence observed in energy proficient cells at 24°C, indicating that the transport of GFP–Dga1 from LDs back to the ER is also energy independent and not inhibited by low temperature, as is the forward transport of Dga1 from the ER to LDs (Fig. 8C; Fig. 6D).

## Discussion

The results presented in this study reveal that LDs can be induced to form from the ER membrane and that such nascent LDs become decorated by integral membrane proteins, which initially are homogenously distributed throughout the ER membrane. Once LDs have been formed, newly synthesized membrane proteins are targeted from the ER to pre-existing LDs and uniformly label the entire LD population. This transport of integral membrane proteins from the ER to LDs does not depend on the COPI or COPII vesicular transport machinery or on vesicle fusion and is independent of temperature and energy. The transport is reversible and results in ER localization of LD-localized membrane proteins upon regression of LDs under lipolytic conditions. This study thus defines a functional relationship between the ER membrane and LDs that allows the bidirectional exchange of integral membrane proteins. The temperature and energy independence of the transport is consistent with a reversible, diffusion-based partitioning of membrane proteins between the ER and LDs, suggesting that the ER membrane is temporally or permanently in continuity with the surface of LDs.

The reversible relocation of membrane proteins between the ER and LDs is not a unique feature of the yeast diacylglycerol acyltransferase and of Erg6, as shown in this study, but is likely to reflect a more general and conserved mechanism to partition membrane proteins between the ER and LDs. The mammalian ortholog of Dga1, DGAT2, for example, relocates from the ER to LDs when cells are treated with fatty acids, indicating that this dual localization of the enzyme is evolutionarily conserved and possibly of functional significance (Kuerschner et al., 2008; Stone et al., 2009). In addition to Dga1/DGAT2, a number of other proteins in both yeast and mammalian cells are dually located in both the ER and on LDs (Goodman, 2009; Leber et al., 1998; Ostermeyer et al., 2001; Zehmer et al., 2009).

How soluble or membrane-anchored proteins are targeted to and retained on LDs is not well understood. LD targeting of both classes of proteins, however, appears to be conserved across species (Hanisch et al., 2006; Kurat et al., 2006; Ting et al., 1997; Zehmer et al., 2008). The mammalian perilipin family members, major soluble LD proteins with conserved structural and functional roles, for example, are probably targeted to the LD surface after they are translated on free ribosomes (Brasaemle et al., 1997). Some of these LD components such as perilipin 1 appear to permanently stay on the LDs but are free to move on the droplet surface, whereas others (i.e. perilipin 2/ADRP and perilipin 5/LSDP5) can freely exchange with a cytosolic pool, as revealed by FRAP analysis (Wang et al., 2009).

By contrast, integral membrane proteins that localize to LDs are first integrated into the ER membrane by translocon-mediated membrane insertion (Beaudoin et al., 2000). How these proteins then relocate from the ER membrane to the surface of LDs, is not well characterized. Many studies that have examined LD targeting of these proteins have concentrated on the identification of the cis-acting sequences that harbor the targeting information rather than on the general mechanism of the targeting pathway. However, analysis of the dynamics of the location of LD-localized membrane proteins, such as caveolin-3, ALDI (associated lipid droplet protein 1), and adipocyte triglyceride lipase (ATGL) in mammalian cells by FRAP revealed they all recover from photobleaching to more than half of the original intensity within 1 hour or less (Pol et al., 2005; Turro et al., 2006; Soni et al., 2009). These data support the notion that membrane proteins dynamically exchange their LD association even though recovery of caveolin-3, ALDI and ATGL is much slower in these systems than we observe with Dga1.

LD targeting of membrane proteins in animal cells is probably best characterized for AAM-B, a putative methyltransferase. AAM-B is first localized to the ER membrane, from where it moves to LDs upon induction of LD formation by oleate supplementation (Zehmer et al., 2008; Zehmer et al., 2009). ER to LD targeting of AAM-B is independent of protein synthesis and not mediated by COPII vesicles, because it is not sensitive to inhibition of Sar1, a small GTPase required for assembly of the COPII vesicular coat (Zehmer et al., 2009). These studies therefore suggested that integral membrane proteins reach LDs by lateral movement from the ER membrane either through a permanent ‘stalk’ type of connection or by transient interactions between the two compartments (Zehmer et al., 2009). Moreover, as observed in the present study with Dga1, AAM-B moves back from LDs into the ER upon induction of lipolysis, indicating that the transport process of integral membrane proteins between the ER and LDs is reversible in both mammalian cells and yeast (Zehmer et al., 2009). Therefore, our results support the conclusions of Zehmer et al., that integral membrane proteins reach LDs by lateral movement from the ER membrane, and extend these findings by showing that transfer from the ER to LDs, as well as the back transport from LDs into the ER membrane, are temperature and energy independent (Zehmer et al., 2009).

Our observations that relocation of Dga1 and Erg6 from the ER to LDs is not significantly delayed in mutants that conditionally block vesicular transport between the ER and Golgi apparatus, by fusion of vesicles with the target membrane, at low temperature, or in energy-depleted cells, all strongly argue against the involvement of a known vesicular transport mechanism in ER to LD targeting of membrane proteins. Defects in vesicular transport, however, affect neutral lipid homeostasis and hence LD formation in both yeast and mice, suggesting that altered localization of some LD components under conditions that impair membrane flow along the secretory pathway might be due to altered LD morphology or to changes in the composition of the limiting membrane (Soni et al., 2009; Beller et al., 2008; Guo et al., 2008; Gaspar et al., 2008; Hommel et al., 2010). By contrast, in vitro studies indicate that membrane proteins might reach LDs through the formation of a novel type of vesicles that is distinct from the ER-derived COPII vesicles (Takeda and Nakano, 2008). Because transport of Dga1 to LDs is independent of protein synthesis, LD targeting of Dga1 can also not be explained by a direct insertion of nascent proteins into the limiting membranes of LDs, as might occur if translocons were localized and functional at the periphery of LDs.

Consistent with a model in which LDs are interconnected with the ER membrane, we find that the transcriptional induction of LD marker proteins, such as Erg6, Tgl1 or Yeh1, results in a uniform labeling of all pre-existing LDs within the cell (supplementary material Fig. S9). Under the conditions analyzed in this study, LDs do not show the properties expected of an independent cytosolic

organelle, i.e. labeling of nascent/ER-associated LDs only, but no labeling of cytosolic LDs upon expression of an LD-localized marker protein. The LDs analyzed here appear to stay connected to the ER membrane and appear not to detach from it, as is proposed by the current biogenetic model (Fujimoto et al., 2008; Murphy and Vance, 1999; Ploegh, 2007).

A close association between the ER membrane and LDs has been observed in a number of different cell types (reviewed by Fujimoto et al., 2008; Goodman, 2009). Live-cell microscopy, for example, revealed close association of LDs with the ER and concurrent movement of both the ER and attached LDs (Targett-Adams et al., 2003). LDs appear to form on ER domains enriched in perilipin 2/ADRP, their apposition with the ER membrane is regulated by the Rab GTPase Rab18 and structurally connected to lipoprotein assembly within the ER lumen (Ohsaki et al., 2008; Ozeki et al., 2005; Robenek et al., 2006). Morphological studies of adipocytes using freeze-fracture electron microscopy revealed that the ER membrane is continuous with the surface layer of LDs (Blanchette-Mackie et al., 1995). Other freeze-fracture studies, however, indicate that LDs are only peripherally associated with the ER membrane (Robenek et al., 2006). Thus, the precise nature and structure of the association between the ER membrane and LDs still need to be defined. In yeast, the majority of the LDs (92–97%) colocalize with an ER marker protein and thus remain closely associated with the ER (Szymanski et al., 2007) (supplementary material Fig. S10). An ER integral membrane protein, Fld1/seipin is localized to the ER–LD junction and seipin mutant cells show aberrantly small and clustered LDs (Fei et al., 2008; Szymanski et al., 2007). Analysis of LD targeting of Dga1 in seipin mutant cells, however, revealed that Dga1 could still move on these aberrant LDs, indicating that seipin is not required to mediate the transfer of integral membrane proteins between the ER and LDs (supplementary material Fig. S11).

The presence of a transient or possibly permanent membrane connection between the ER and LDs, as indicated by the results of this study, could not only explain the partitioning of membrane proteins between the two compartments, but it could also account for the exchange of lipids between the ER and LDs. Bidirectional transport of lipids between the ER and LDs must occur under lipogenic conditions, when LDs form and grow, and during lipolysis, when LDs regress. During lipogenesis neutral lipids are synthesized by enzymes with homogenous ER localization, such as Lro1, Are1 and Are2, and by the dually located Dga1 (Oelkers et al., 2002; Sorger and Daum, 2002; Zweytick et al., 2000). To support LD growth, the neutral lipids generated by these ER-localized enzymes need either to be transported to LDs or generated locally by LD-localized Dga1/DGAT2 (Cheng et al., 2009; Kuerschner et al., 2008; Sorger and Daum, 2002). Because membranes can adsorb neutral lipids to up to 4 mol%, transport of neutral lipids from their site of synthesis to the storage compartment could take place through a membrane that connects the ER to LDs (Hamilton et al., 1983). Thus the ER membrane might not only act as a source of neutral lipids but might itself also provide the transport route for these lipids to reach LDs. This concept is supported by the observation that photobleaching of LDs loaded with a fluorescent cholesterol analogue, BODIPY-cholesterol, results in very rapid recovery of fluorescence ($\leq$ 1 minute) after bleaching, presumably through an ER-mediated supply of cholesterol to the LDs (Jansen et al., 2011). At LDs, neutral lipids might be removed from the connecting membrane by partitioning into the hydrophobic core of the droplet, which would shift the equilibrium towards LD growth (Cheng et al., 2009; Kuerschner et al., 2008).

Membrane continuity between ER and LDs could also account for the reverse process, i.e. the back transport of lipids from LDs to the ER during lipolysis. Under these conditions, LD-localized lipases hydrolyze TAG and steryl esters to liberate free fatty acids, diacylglycerol and free sterols. These lipid intermediates are water insoluble but could be released from LDs into the connecting ER membrane and thus enter the pool of lipids that are synthesized de novo by the ER-localized lipid biosynthetic enzymes.

If membrane proteins are free to partition between the ER and LDs by lateral diffusion as suggested by the results shown here, one might wonder what determines the relative abundance of a given protein in the ER relative to that on LDs. The observation that some LD-localized membrane proteins, such as Erg6, were concentrated on LDs while they were forming in the ER, whereas others, such as Dga1, remained in the ER and moved to LDs only after some time, further indicates that proteins differ in their residence time in the ER. Partitioning of membrane proteins between the ER and LDs might depend on signals that are present on LDs, such as specific proteins or differences in the lipid composition of the membrane that is in close proximity to these neutral lipid depots. Differences in affinities for these signals could explain why Dga1 moved to LDs only after Erg6 was already present on these structures. This notion is supported by the observation that the perilipin family protein 3/Tip47 is targeted to diacylglycerol-rich membranes (Skinner et al., 2009). Diacylglycerol is the immediate biochemical precursor for the TAG contained within LDs, and is also present in isolated LDs (Kuerschner et al., 2008). Thus lipid-mediated sorting of proteins to LDs or TAG-rich ER membrane domains seems a relevant hypothesis to test.

LDs are generally thought to be enclosed by an unusual lipid monolayer rather than a bilayer membrane as found on other organelles (Murphy and Vance, 1999; Tauchi-Sato et al., 2002). The integral membrane proteins whose targeting was analyzed in this study, i.e. Dga1, Tgl1 and Yeh1, however, all have predicted transmembrane domains that are long enough to span a normal membrane bilayer. However, there are other integral membrane proteins that localize to LDs that contain a hairpin-type of membrane anchor, as present in the plant oleosins and in caveolin (Abell et al., 2004; Ingelmo-Torres et al., 2009). The fact that Dga1 is enzymatically active in both microsomes and isolated LDs, indicates that the localization and membrane environment of the enzyme does not grossly affect its activity and hence most likely also preserves the structure of the protein (Oelkers et al., 2002; Sorger and Daum, 2002). The membrane topology of Dga1 and that of its mammalian and plant ortholog DGAT2 indicates that both N- and C-terminal ends are located in the cytosol and that the protein spans the membrane twice, in a hairpin-type of topology (Shockey et al., 2006; Stone et al., 2006) (supplementary material Fig. S4). It is conceivable that this particular topology of Dga1 and of other LD-localized membrane proteins is compatible with their native insertion into a bilayer as well as a monolayer membrane.

The question of how these membrane proteins move from the normal bilayer membrane of the ER onto a possible lipid monolayer that is thought to limit the surface of LDs can only be speculated on at this time. Our observations, however, that this transport occurs fast, is energy and temperature independent, subject to temporal control and can occur in both directions, are all consistent with the proposal that the ER membrane is continuous with the surface of the LD (Fig. 9). Transient or permanent continuity between the ER membrane and the LD

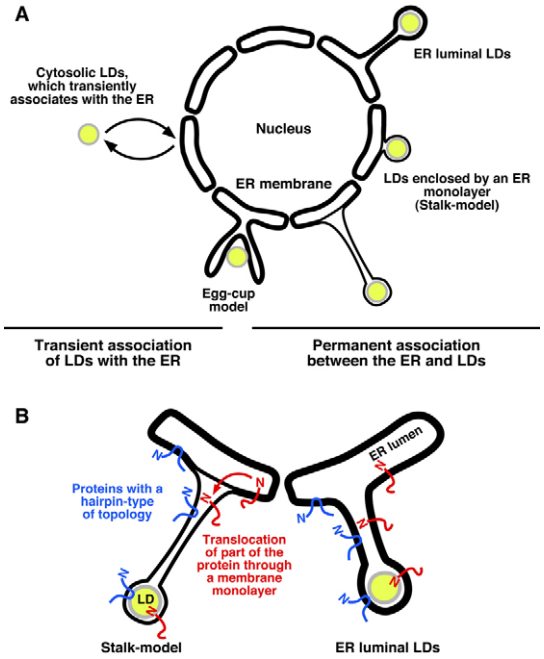


**Fig. 9. Possible association between the ER membrane and LDs to facilitate the bidirectional exchange of integral membrane proteins between the two compartments.** (**A**) Models for the transient or permanent association between the ER membrane and LDs. Depicted are cytosolic LDs, which transiently interact with the surface of the ER membrane, an ER membrane holding an LD as proposed in the egg-cup model by Robenek et al., an extended membrane stalk enclosing the LD as proposed by Zehmer et al., a modified stalk model to account for the high degree of colocalization of LDs with the ER membrane in yeast, and a model in which LDs would be located in the ER lumen and enclosed by the ER bilayer membrane (Robenek et al., 2006; Zehmer et al., 2009). (**B**) Translocation of integral membrane proteins between the ER and LDs. A diffusion-based transfer of membrane proteins with a hairpin-type of topology is depicted in blue. By contrast the integral membrane protein in red, which has an ER-lumenal domain, needs to transfer its lumenal domain across a membrane monolayer in the stalk-model (red arrow). If LDs were located in the ER lumen, however, all classes of integral membrane proteins could reversibly partition between a homogenous ER distribution and a punctate LD localization. Thin lines represent a lipid monolayer, whereas thick lines represent a bilayer membrane.

surface has been proposed to account for the bidirectional transport of AAM-B between the ER and LDs (Zehmer et al., 2009). The observation that transcriptional induction of LD-localized membrane proteins results in uniform labeling of all LDs, indicates that the association of LDs with the ER is either permanent or that it occurs frequently enough to result in an uniform transfer of proteins between the surface of the two compartments. Membrane continuity through a stalk-like connection could account for the lateral partitioning of membrane proteins with a hairpin-type topology between the ER bilayer and an LD monolayer, as proposed by Zehmer et al. (Zehmer et al., 2009). How proteins that have an ER lumenal domain, such as Tgl1, could cross the interface between the two compartments is less clear (Koffel et al., 2005) (supplementary material Fig. S2, Fig. S9B). In the stalk model, transfer of Tgl1 from the ER bilayer onto an LD monolayer would require that the ER lumenal domain of the protein crosses the inner leaflet of the ER membrane, a process that is unlikely to occur spontaneously (Fig. 9B, red arrow). These topological problems could be resolved if LDs were formed in the ER membrane and then bud into the ER lumenal compartment rather than into the cytosol. In such a model, the ER lumenally localized LD would be surrounded by the ER bilayer membrane and the close apposition of LDs with the ER membrane could define a lateral domain of the ER within which LD-localized membrane proteins could concentrate, irrespective of their topology, by simple lateral segregation. This model predicts that, in vivo, LDs are enclosed by a bilayer membrane that is continuous with the ER. Although this is not in agreement with many morphological studies by electron microscopy, mostly of chemically fixed cells, which did not resolve a bilayer membrane at the periphery of LDs, the negative evidence provided by these investigations might need to be re-evaluated using novel complementary and functional approaches (Murphy, 2001). LDs have a very unusual chemical composition with a high concentration of neutral lipids not only in the LD itself but possibly also in the adjacent ER domain. This might render the structure particularly sensitive to the fixation and the contrast-producing methods routinely used for electron microscopy, making it difficult to ensure preservation of the native structure and to resolve the nature of the membrane connecting to or possibly enclosing the structure (DiDonato and Brasaemle, 2003; Belazi et al., 2009).

## Materials and Methods

### Yeast strains and growth conditions

Yeast strains and their genotypes are listed in supplementary material Table S1. Strains were cultured in YP-rich medium [1% Bacto yeast extract, 2% Bacto peptone (USBiological, Swampscott, MA)] or minimal medium [0.67% yeast nitrogen base without amino acids (USBiological), 0.73 g/l amino acids)], containing either 2% glucose, galactose or raffinose. Double- and triple-mutant strains were generated by crossing of single mutants and by gene disruption, using PCR deletion cassettes and a marker rescue strategy (Gueldener et al., 2002; Longtine et al., 1998).

### GFP-tagging, subcellular fractionation and western blot analysis

Promoter replacement, GFP- and epitope-tagging were performed by homologous recombination using PCR fusion cassettes, and correct integration of the fusion cassette was confirmed by colony PCR (Longtine et al., 1998).

Protein concentrations were determined using the Folin reagent and BSA as standard. Proteins were precipitated with 10% trichloroacetic acid (TCA), resuspended in sample buffer and separated by SDS-polyacrylamide gel electrophoresis. Western blots were probed with rabbit antisera against GFP (1:5000; Torrey Pines Biolabs, Inc., Huston, TX), Kar2 (1:5000; M. Rose, Princeton University), Wbp1 (1:1000, M. Aebi, Eidgenössische Technische Hochschule University, Zurich, Switzerland), Ayr1 (1:5000; G. Daum, Graz University of Technology, Austria) or mouse anti-myc antibody (1:500; Zymed Laboratories Inc., South San Francisco, CA).

Differential fractionation, determination of membrane association, topology and glycosylation of epitope-tagged Dga1 were performed as previously described (Koffel et al., 2005). Pulse–chase analysis to monitor maturation of carboxypeptidase Y was performed as described previously (Munn et al., 1999).

### Lipid labeling

TAG synthesis upon induction of Lro1 and Dga1 was analyzed by labeling the neutral lipid pool with [$^3$H]palmitic acid. *GAL-LRO1* and *GAL-DGA1* strains were cultured in YP–raffinose medium, diluted and resuspended in YPD or YP–galactose media and grown in the presence of 10 µCi/ml [9,10-$^3$H]palmitic acid (10 mCi/ml; American Radiolabeled Chemicals, Inc., St Louis, MO). Cells were collected, lipids were extracted with chloroform–methanol (1:1; vol./vol.), and equal aliquots were brought to dryness. Lipids were separated by thin-layer chromatography (TLC) on silica gel 60 plates (Merck, Darmstadt, Germany), developed in petroleum ether–diethylether–acetic acid (70:30:2; per vol.), and quantified by scanning with a Berthold Tracemaster 20 Automatic TLC-Linear Analyzer (Berthold Technologies, Bad Wildbach, Germany). TLC plates were then exposed to a tritium-sensitive screen and visualized using a phosphorimager (Bio-Rad Laboratories, Hercules, CA).

TAG mobilization was monitored in cells that were labeled with 10 µCi/ml [$^3$H]palmitic acid in galactose-containing medium, overnight, and then diluted into fresh glucose-containing medium supplemented with cerulenin (10 µg/ml).

### Isolation of LDs

LDs were isolated by three consecutive flotations essentially as described previously (Leber et al., 1994). Briefly, spheroplasts were resuspended in lysis buffer (12%

Ficoll PM 400, 10 mM MES–Tris, pH 6.9, 0.2 mM EDTA) and the lysate was cleared by centrifugation at 5000 ***g*** for 5 minutes. This homogenate (H) was placed at the bottom of an ultracentrifuge tube, overlaid with lysis buffer and subjected to flotation by centrifugation at 100,000 ***g*** for 1 hour. The floating fraction (F1) was collected, diluted with lysis buffer and placed at the bottom of a second ultracentrifuge tube. The sample was overlaid with 8% Ficoll in 10 mM MES–Tris, pH 6.9, 0.2 mM EDTA and centrifuged again at 100,000 ***g*** for 1 hour. The second floating fraction (F2) was collected, diluted with 0.6 M sorbitol in 8% Ficoll, 10 mM MES–Tris, pH 6.9, 0.2 mM EDTA. The sample was then placed at the bottom of a third ultracentrifuge tube overlaid with 0.25 M sorbitol in MES–Tris, pH 6.9, 0.2 mM EDTA and again subjected to flotation by centrifugation at 100,000 ***g*** for 1 hour. The film floating on this third gradient (F3) is the LD-containing fraction.

### Confocal microscopy

LDs were stained with BODIPY 493/503 (1 μg/ml; Invitrogen, Carlsbad, CA) for 30 minutes at room temperature and cells were washed twice with PBS containing 50 μM fatty-acid-free BSA and once with PBS. Cells were stained with Nile Red (10 μg/ml; Sigma-Aldrich, St Louis, MO) for 1 minute at 24°C and washed twice with PBS. For staining with FM4-64, early logarithmic cells were concentrated to 10 OD units of cells/ml and incubated with 32 μM FM4-64 (Invitrogen) for 30 minutes on ice. Cells were then poisoned and incubated at room temperature for 30 minutes or kept on ice. Cycloheximide was used at 50 μg/ml, $NaN_3$ and NaF at 20 mM each.

Fluorescence microscopy was used to detect GFP- and RFP-tagged proteins in living cells using a Leica TCS SP5 confocal microscope with LAS AF software. All images were recorded with a 63×/1.20 HCX PL APO objective at a zoom of 6. Results from double labeling experiments were recorded with the following settings. For sequential recording of GFP and Nile Red fluorescence, GFP was exited at 476 nm and emission was recorded from 490–517 nm; Nile Red was excited at 561 nm and emission was recorded from 580–660 nm. For recording of GFP and RFP fluorescence, GFP was excited at 476 nm and recorded from 490–560 nm; RFP was excited at 561 nm and emission was recorded from 580–660 nm. Photobleaching experiments were performed using the FRAP wizard in LAS AF with activated FlyMode to measure fluorescence during bleaching. Bleaching time was 12 seconds for FRAP experiments and images were recorded every 20 seconds during recovery. Quantification of the FRAP and FLIP results was performed as described previously (Ellenberg et al., 1997; Lippincott-Schwartz et al., 2001).

### Electron microscopy

For IEM, cells were grown in raffinose-containing medium, shifted to galactose-containing medium, and further incubated at 24°C. Aliquots were collected after 0, 4, 8 and 24 hours before being chemically fixed, embedded in 12% gelatin and cryosectioned as described previously (Griffith et al., 2008). Sections were then immunogold-labeled using a rabbit anti-GFP antiserum (Abcam, Cambridge, UK) and 10 nm protein A–gold before being viewed in a JEOL 1010 electron microscope (JEOL, Tokyo, Japan).

For the statistical evaluations, the number of lipid droplets per cell section was determined by counting 100 randomly selected cell profiles for each time point. The relative distribution of the gold particles at each time point was calculated by classifying 550 of them, on the basis of their localization to the ER, LDs and mitochondria. A gold particle was assigned to a compartment when it was situated within 25 nm of the limiting membrane. The linear labeling density and the average organelle surface were established using the point hit method as described previously (Kondylis and Rabouille, 2003; Rabouille, 1999). Standard deviations were used to perform a *t*-test, confirming the statistical significance of the data ($P<0.05$).

For morphological analyses of cryofixed cells, cells were centrifuged and transferred into membrane platelets and frozen by high-pressure freezing (Leica EMPACT2, Leica-Microsystems, Vienna, Austria) (Studer et al., 2001). The frozen specimens were freeze-substituted in acetone containing 2% osmium tetroxide, 0.1% uranyl acetate and 3% water (AFS; Leica-Microsystems) (Walther and Ziegler, 2002) and embedded in Epon Araldite. Samples were substituted at –90°C, for 27 hours, at –60°C for 8 hours and at –30°C for another 8 hours. They were then warmed to 4°C, washed three times for 10 minutes in 100% acetone and embedded in Epon 812 (30%, 70%, 100%). Blocks were polymerized at 60°C for 5 days. Semithin and ultrathin sections were collected on 200 mesh grids, post stained with uranyl acetate and lead citrate, and visualized with a Philips CM-100 electron microscope, operating at 80 kV. Images were recorded on a side-mounted digital camera (Morada Soft Imaging System, Olympus) and processed with iTEM software.

We thank R. Köffel for fruitful discussions that lead to the initiation of this project, D. Studer for help in electron microscopy, and A. Spang for mutant yeast strains. This work was supported by the Netherlands Organization for Health Research and Development (ZonMW-VIDI-917.76.329 to F.R.), the Netherlands Organization for Scientific Research (Chemical Sciences, ECHO grant-700.59.003 to F.R.), the Utrecht University (High Potential grant to F.R.), the Novartis Foundation (08A09 to R.S.) and the Swiss National Science Foundation (PP00A-110450 and 3100-120650 to R.S.).

Supplementary material available online at
http://jcs.biologists.org/cgi/content/full/124/14/2424/DC1

## References

**Abell, B. M., Hahn, M., Holbrook, L. A. and Moloney, M. M.** (2004). Membrane topology and sequence requirements for oil body targeting of oleosin. *Plant J.* **37**, 461-470.

**Athenstaedt, K. and Daum, G.** (2000). 1-Acyldihydroxyacetone-phosphate reductase (Ayr1p) of the yeast Saccharomyces cerevisiae encoded by the open reading frame YIL124w is a major component of lipid particles. *J. Biol. Chem.* **275**, 235-240.

**Beaudoin, F., Wilkinson, B. M., Stirling, C. J. and Napier, J. A.** (2000). In vivo targeting of a sunflower oil body protein in yeast secretory (sec) mutants. *Plant J.* **23**, 159-170.

**Belazi, D., Sole-Domenech, S., Johansson, B., Schalling, M. and Sjovall, P.** (2009). Chemical analysis of osmium tetroxide staining in adipose tissue using imaging ToF-SIMS. *Histochem. Cell Biol.* **132**, 105-115.

**Beller, M., Sztalryd, C., Southall, N., Bell, M., Jackle, H., Auld, D. S. and Oliver, B.** (2008). COPI complex is a regulator of lipid homeostasis. *PLoS Biol.* **6**, e292.

**Blanchette-Mackie, E. J., Dwyer, N. K., Barber, T., Coxey, R. A., Takeda, T., Rondinone, C. M., Theodorakis, J. L., Greenberg, A. S. and Londos, C.** (1995). Perilipin is located on the surface layer of intracellular lipid droplets in adipocytes. *J. Lipid Res.* **36**, 1211-1226.

**Brasaemle, D. L., Barber, T., Kimmel, A. R. and Londos, C.** (1997). Post-translational regulation of perilipin expression. Stabilization by stored intracellular neutral lipids. *J. Biol. Chem.* **272**, 9378-9387.

**Cheng, J., Fujita, A., Ohsaki, Y., Suzuki, M., Shinohara, Y. and Fujimoto, T.** (2009). Quantitative electron microscopy shows uniform incorporation of triglycerides into existing lipid droplets. *Histochem. Cell Biol.* **132**, 281-291.

**Czabany, T., Athenstaedt, K. and Daum, G.** (2007). Synthesis, storage and degradation of neutral lipids in yeast. *Biochim. Biophys. Acta* **1771**, 299-309.

**Dahlqvist, A., Stahl, U., Lenman, M., Banas, A., Lee, M., Sandager, L., Ronne, H. and Stymne, S.** (2000). Phospholipid:diacylglycerol acyltransferase: an enzyme that catalyzes the acyl-CoA-independent formation of triacylglycerol in yeast and plants. *Proc. Natl. Acad. Sci. USA* **97**, 6487-6492.

**DiDonato, D. and Brasaemle, D. L.** (2003). Fixation methods for the study of lipid droplets by immunofluorescence microscopy. *J. Histochem. Cytochem.* **51**, 773-780.

**Ducharme, N. A. and Bickel, P. E.** (2008). Lipid droplets in lipogenesis and lipolysis. *Endocrinology* **149**, 942-949.

**Ellenberg, J., Siggia, E. D., Moreira, J. E., Smith, C. L., Presley, J. F., Worman, H. J. and Lippincott-Schwartz, J.** (1997). Nuclear membrane dynamics and reassembly in living cells: targeting of an inner nuclear membrane protein in interphase and mitosis. *J. Cell Biol.* **138**, 1193-1206.

**Fei, W., Shui, G., Gaeta, B., Du, X., Kuerschner, L., Li, P., Brown, A. J., Wenk, M. R., Parton, R. G. and Yang, H.** (2008). Fld1p, a functional homologue of human seipin, regulates the size of lipid droplets in yeast. *J. Cell Biol.* **180**, 473-482.

**Fujimoto, T., Ohsaki, Y., Cheng, J., Suzuki, M. and Shinohara, Y.** (2008). Lipid droplets: a classic organelle with new outfits. *Histochem. Cell Biol.* **130**, 263-279.

**Gao, X. D., Tachikawa, H., Sato, T., Jigami, Y. and Dean, N.** (2005). Alg14 recruits Alg13 to the cytoplasmic face of the endoplasmic reticulum to form a novel bipartite UDP-N-acetylglucosamine transferase required for the second step of N-linked glycosylation. *J. Biol. Chem.* **280**, 36254-36262.

**Gaspar, M. L., Jesch, S. A., Viswanatha, R., Antosh, A. L., Brown, W. J., Kohlwein, S. D. and Henry, S. A.** (2008). A block in endoplasmic reticulum-to-Golgi trafficking inhibits phospholipid synthesis and induces neutral lipid accumulation. *J. Biol. Chem.* **283**, 25735-25751.

**Gocze, P. M. and Freeman, D. A.** (1994). Factors underlying the variability of lipid droplet fluorescence in MA-10 Leydig tumor cells. *Cytometry* **17**, 151-158.

**Goodman, J. M.** (2009). Demonstrated and inferred metabolism associated with cytosolic lipid droplets. *J. Lipid Res.* **50**, 2148-2156.

**Griffith, J., Mari, M., De Maziere, A. and Reggiori, F.** (2008). A cryosectioning procedure for the ultrastructural analysis and the immunogold labelling of yeast Saccharomyces cerevisiae. *Traffic* **9**, 1060-1072.

**Gueldener, U., Heinisch, J., Koehler, G. J., Voss, D. and Hegemann, J. H.** (2002). A second set of loxP marker cassettes for Cre-mediated multiple gene knockouts in budding yeast. *Nucleic Acids Res.* **30**, e23.

**Guo, Y., Walther, T. C., Rao, M., Stuurman, N., Goshima, G., Terayama, K., Wong, J. S., Vale, R. D., Walter, P. and Farese, R. V.** (2008). Functional genomic screen reveals genes involved in lipid-droplet formation and utilization. *Nature* **453**, 657-661.

**Hamilton, J. A., Miller, K. W. and Small, D. M.** (1983). Solubilization of triolein and cholesteryl oleate in egg phosphatidylcholine vesicles. *J. Biol. Chem.* **258**, 12821-12826.

**Hanisch, J., Waltermann, M., Robenek, H. and Steinbuchel, A.** (2006). Eukaryotic lipid body proteins in oleogenous actinomycetes and their targeting to intracellular triacylglycerol inclusions: impact on models of lipid body biogenesis. *Appl. Environ. Microbiol.* **72**, 6743-6750.

**Hommel, A., Hesse, D., Volker, W., Jaschke, A., Moser, M., Engel, T., Bluher, M., Zahn, C., Chadt, A., Ruschke, K. et al.** (2010). The ARF-like GTPase ARFRP1 is essential for lipid droplet growth and is involved in the regulation of lipolysis. *Mol. Cell. Biol.* **30**, 1231-1242.

**Hope, R. G., Murphy, D. J. and McLauchlan, J.** (2002). The domains required to direct core proteins of hepatitis C virus and GB virus-B to lipid droplets share common features with plant oleosin proteins. *J. Biol. Chem.* **277**, 4261-4270.

**Ingelmo-Torres, M., Gonzalez-Moreno, E., Kassan, A., Hanzal-Bayer, M., Tebar, F., Herms, A., Grewal, T., Hancock, J. F., Enrich, C., Bosch, M. et al.** (2009). Hydrophobic and basic domains target proteins to lipid droplets. *Traffic* **10**, 1785-1801.

**Jansen, M., Ohsaki, Y., Rita Rega, L., Bittman, R., Olkkonen, V. M. and Ikonen, E.** (2011). Role of ORPs in sterol transport from plasma membrane to ER and lipid droplets in mammalian cells. *Traffic* **12**, 218-231.

**Kalantari, F., Bergeron, J. J. and Nilsson, T.** (2010). Biogenesis of lipid droplets - how cells get fatter. *Mol. Membr. Biol.* **27**, 462-468.

**Koffel, R., Tiwari, R., Falquet, L. and Schneiter, R.** (2005). The Saccharomyces cerevisiae YLL012/YEH1, YLR020/YEH2, and TGL1 genes encode a novel family of membrane-anchored lipases that are required for steryl ester hydrolysis. *Mol. Cell. Biol.* **25**, 1655-1668.

**Kondylis, V. and Rabouille, C.** (2003). A novel role for dp115 in the organization of tER sites in Drosophila. *J. Cell Biol.* **162**, 185-198.

**Kuerschner, L., Moessinger, C. and Thiele, C.** (2008). Imaging of lipid biosynthesis: how a neutral lipid enters lipid droplets. *Traffic* **9**, 338-352.

**Kurat, C. F., Natter, K., Petschnigg, J., Wolinski, H., Scheuringer, K., Scholz, H., Zimmermann, R., Leber, R., Zechner, R. and Kohlwein, S. D.** (2006). Obese yeast: triglyceride lipolysis is functionally conserved from mammals to yeast. *J. Biol. Chem.* **281**, 491-500.

**Leber, R., Zinser, E., Zellnig, G., Paltauf, F. and Daum, G.** (1994). Characterization of lipid particles of the yeast, Saccharomyces cerevisiae. *Yeast* **10**, 1421-1428.

**Leber, R., Landl, K., Zinser, E., Ahorn, H., Spok, A., Kohlwein, S. D., Turnowsky, F. and Daum, G.** (1998). Dual localization of squalene epoxidase, Erg1p, in yeast reflects a relationship between the endoplasmic reticulum and lipid particles. *Mol. Biol. Cell* **9**, 375-386.

**Lippincott-Schwartz, J., Snapp, E. and Kenworthy, A.** (2001). Studying protein dynamics in living cells. *Nat. Rev. Mol. Cell Biol.* **2**, 444-456.

**Longtine, M. S., Mckenzie, A., 3rd, Demarini, D. J., Shah, N. G., Wach, A., Brachat, A., Philippsen, P. and Pringle, J. R.** (1998). Additional modules for versatile and economical PCR-based gene deletion and modification in Saccharomyces cerevisiae. *Yeast* **14**, 953-961.

**Malinska, K., Malinsky, J., Opekarova, M. and Tanner, W.** (2004). Distribution of Can1p into stable domains reflects lateral protein segregation within the plasma membrane of living *S. cerevisiae* cells. *J. Cell Sci.* **117**, 6031-6041.

**Mullner, H., Zweytick, D., Leber, R., Turnowsky, F. and Daum, G.** (2004). Targeting of proteins involved in sterol biosynthesis to lipid particles of the yeast Saccharomyces cerevisiae. *Biochim. Biophys. Acta* **1663**, 9-13.

**Munn, A. L., Heese-Peck, A., Stevenson, B. J., Pichler, H. and Riezman, H.** (1999). Specific sterols required for the internalization step of endocytosis in yeast. *Mol. Biol. Cell* **10**, 3943-3957.

**Murphy, D. J.** (2001). The biogenesis and functions of lipid bodies in animals, plants and microorganisms. *Prog. Lipid Res.* **40**, 325-438.

**Murphy, D. J. and Vance, J.** (1999). Mechanisms of lipid-body formation. *Trends Biochem. Sci.* **24**, 109-115.

**Nikonov, A. V., Snapp, E., Lippincott-Schwartz, J. and Kreibich, G.** (2002). Active translocon complexes labeled with GFP-Dad1 diffuse slowly as large polysome arrays in the endoplasmic reticulum. *J. Cell Biol.* **158**, 497-506.

**Oelkers, P., Tinkelenberg, A., Erdeniz, N., Cromley, D., Billheimer, J. T. and Sturley, S. L.** (2000). A lecithin cholesterol acyltransferase-like gene mediates diacylglycerol esterification in yeast. *J. Biol. Chem.* **275**, 15609-15612.

**Oelkers, P., Cromley, D., Padamsee, M., Billheimer, J. T. and Sturley, S. L.** (2002). The DGA1 gene determines a second triglyceride synthetic pathway in yeast. *J. Biol. Chem.* **277**, 8877-8881.

**Ohsaki, Y., Cheng, J., Suzuki, M., Fujita, A. and Fujimoto, T.** (2008). Lipid droplets are arrested in the ER membrane by tight binding of lipidated apolipoprotein B-100. *J. Cell Sci.* **121**, 2415-2422.

**Olofsson, S. O., Bostrom, P., Andersson, L., Rutberg, M., Perman, J. and Boren, J.** (2009). Lipid droplets as dynamic organelles connecting storage and efflux of lipids. *Biochim. Biophys. Acta* **1791**, 448-458.

**Ostermeyer, A. G., Paci, J. M., Zeng, Y., Lublin, D. M., Munro, S. and Brown, D. A.** (2001). Accumulation of caveolin in the endoplasmic reticulum redirects the protein to lipid storage droplets. *J. Cell Biol.* **152**, 1071-1078.

**Ozeki, S., Cheng, J., Tauchi-Sato, K., Hatano, N., Taniguchi, H. and Fujimoto, T.** (2005). Rab18 localizes to lipid droplets and induces their close apposition to the endoplasmic reticulum-derived membrane. *J. Cell Sci.* **118**, 2601-2611.

**Ploegh, H. L.** (2007). A lipid-based model for the creation of an escape hatch from the endoplasmic reticulum. *Nature* **448**, 435-438.

**Pol, A., Martin, S., Fernandez, M. A., Ingelmo-Torres, M., Ferguson, C., Enrich, C. and Parton, R. G.** (2005). Cholesterol and fatty acids regulate dynamic caveolin trafficking through the Golgi complex and between the cell surface and lipid bodies. *Mol. Biol. Cell* **16**, 2091-2105.

**Rabouille, C.** (1999). Quantitative aspects of immunogold labeling in embedded and nonembedded sections. *Methods Mol. Biol.* **117**, 125-144.

**Robenek, H., Hofnagel, O., Buers, I., Robenek, M. J., Troyer, D. and Severs, N. J.** (2006). Adipophilin-enriched domains in the ER membrane are sites of lipid droplet biogenesis. *J. Cell Sci.* **119**, 4215-4224.

**Robenek, H., Buers, I., Hofnagel, O., Robenek, M. J., Troyer, D. and Severs, N. J.** (2009). Compartmentalization of proteins in lipid droplet biogenesis. *Biochim. Biophys. Acta* **1791**, 408-418.

**Sandager, L., Gustavsson, M. H., Stahl, U., Dahlqvist, A., Wiberg, E., Banas, A., Lenman, M., Ronne, H. and Stymne, S.** (2002). Storage lipid synthesis is non-essential in yeast. *J. Biol. Chem.* **277**, 6478-6482.

**Schneiter, R., Brugger, B., Sandhoff, R., Zellnig, G., Leber, A., Lampl, M., Athenstaedt, K., Hrastnik, C., Eder, S., Daum, G. et al.** (1999). Electrospray ionization tandem mass spectrometry (ESI-MS/MS) analysis of the lipid molecular species composition of yeast subcellular membranes reveals acyl chain-based sorting/remodeling of distinct molecular species en route to the plasma membrane. *J. Cell Biol.* **146**, 741-754.

**Shockey, J. M., Gidda, S. K., Chapital, D. C., Kuan, J. C., Dhanoa, P. K., Bland, J. M., Rothstein, S. J., Mullen, R. T. and Dyer, J. M.** (2006). Tung tree DGAT1 and DGAT2 have nonredundant functions in triacylglycerol biosynthesis and are localized to different subdomains of the endoplasmic reticulum. *Plant Cell* **18**, 2294-2313.

**Skinner, J. R., Shew, T. M., Schwartz, D. M., Tzekov, A., Lepus, C. M., Abumrad, N. A. and Wolins, N. E.** (2009). Diacylglycerol enrichment of endoplasmic reticulum or lipid droplets recruits perilipin 3/TIP47 during lipid storage and mobilization. *J. Biol. Chem.* **284**, 30941-30948.

**Soni, K. G., Mardones, G. A., Sougrat, R., Smirnova, E., Jackson, C. L. and Bonifacino, J. S.** (2009). Coatomer-dependent protein delivery to lipid droplets. *J. Cell Sci.* **122**, 1834-1841.

**Sorger, D. and Daum, G.** (2002). Synthesis of triacylglycerols by the acyl-coenzyme A:diacyl-glycerol acyltransferase Dga1p in lipid particles of the yeast Saccharomyces cerevisiae. *J. Bacteriol.* **184**, 519-524.

**Sorger, D., Athenstaedt, K., Hrastnik, C. and Daum, G.** (2004). A yeast strain lacking lipid particles bears a defect in ergosterol formation. *J. Biol. Chem.* **279**, 31190-31196.

**Stone, S. J., Levin, M. C. and Farese, R. V. J.** (2006). Membrane topology and identification of key functional amino acid residues of murine acyl-CoA:diacylglycerol acyltransferase-2. *J. Biol. Chem.* **281**, 40273-40282.

**Stone, S. J., Levin, M. C., Zhou, P., Han, J., Walther, T. C. and Farese, R. V. J.** (2009). The endoplasmic reticulum enzyme DGAT2 is found in mitochondria-associated membranes and has a mitochondrial targeting signal that promotes its association with mitochondria. *J. Biol. Chem.* **284**, 5352-5361.

**Studer, D., Graber, W., Al-Amoudi, A. and Eggli, P.** (2001). A new approach for cryofixation by high-pressure freezing. *J. Microsc.* **203**, 285-294.

**Subramanian, V., Garcia, A., Sekowski, A. and Brasaemle, D. L.** (2004). Hydrophobic sequences target and anchor perilipin A to lipid droplets. *J. Lipid Res.* **45**, 1983-1991.

**Szymanski, K. M., Binns, D., Bartz, R., Grishin, N. V., Li, W. P., Agarwal, A. K., Garg, A., Anderson, R. G. and Goodman, J. M.** (2007). The lipodystrophy protein seipin is found at endoplasmic reticulum lipid droplet junctions and is important for droplet morphology. *Proc. Natl. Acad. Sci. USA* **104**, 20890-20895.

**Takeda, Y. and Nakano, A.** (2008). In vitro formation of a novel type of membrane vesicles containing Dpm1p: putative transport vesicles for lipid droplets in budding yeast. *J. Biochem.* **143**, 803-811.

**Targett-Adams, P., Chambers, D., Gledhill, S., Hope, R. G., Coy, J. F., Girod, A. and McLauchlan, J.** (2003). Live cell analysis and targeting of the lipid droplet-binding adipocyte differentiation-related protein. *J. Biol. Chem.* **278**, 15998-16007.

**Tauchi-Sato, K., Ozeki, S., Houjou, T., Taguchi, R. and Fujimoto, T.** (2002). The surface of lipid droplets is a phospholipid monolayer with a unique fatty acid composition. *J. Biol. Chem.* **277**, 44507-44512.

**Ting, J. T., Balsamo, R. A., Ratnayake, C. and Huang, A. H.** (1997). Oleosin of plant seed oil bodies is correctly targeted to the lipid bodies in transformed yeast. *J. Biol. Chem.* **272**, 3699-3706.

**Tokuyasu, K. T.** (1973). A technique for ultracryotomy of cell suspensions and tissues. J. Cell Biol. **57**, 551-565.

**Turro, S., Ingelmo-Torres, M., Estanyol, J. M., Tebar, F., Fernandez, M. A., Albor, C. V., Gaus, K., Grewal, T., Enrich, C. and Pol, A.** (2006). Identification and characterization of associated with lipid droplet protein 1, A novel membrane-associated protein that resides on hepatic lipid droplets. *Traffic* **7**, 1254-1269.

**van Drogen, F., Stucke, V. M., Jorritsma, G. and Peter, M.** (2001). MAP kinase dynamics in response to pheromones in budding yeast. *Nat. Cell Biol.* **3**, 1051-1059.

**Vida, T. A. and Emr, S. D.** (1995). A new vital stain for visualizing vacuolar membrane dynamics and endocytosis in yeast. *J. Cell Biol.* **128**, 779-792.

**Waltermann, M., Hinz, A., Robenek, H., Troyer, D., Reichelt, R., Malkus, U., Galla, H. J., Kalscheuer, R., Stoveken, T., von Landenberg, P. and Steinbuchel, A.** (2005). Mechanism of lipid-body formation in prokaryotes: how bacteria fatten up. *Mol. Microbiol.* **55**, 750-763.

**Walther, P. and Ziegler, A.** (2002). Freeze substitution of high-pressure frozen samples: the visibility of biological membranes is improved when the substitution medium contains water. *J. Microsc.* **208**, 3-10.

**Wang, H., Hu, L., Dalen, K., Dorward, H., Marcinkiewicz, A., Russell, D., Gong, D., Londos, C., Yamaguchi, T., Holm, C. et al.** (2009). Activation of hormone-sensitive lipase requires two steps, protein phosphorylation and binding to the PAT-1 domain of lipid droplet coat proteins. *J. Biol. Chem.* **284**, 32116-32125.

**Welte, M. A.** (2007). Proteins under new management: lipid droplets deliver. *Trends Cell Biol.* **17**, 363-339.

**Zehmer, J. K., Bartz, R., Liu, P. and Anderson, R. G.** (2008). Identification of a novel N-terminal hydrophobic sequence that targets proteins to lipid droplets. *J. Cell Sci.* **121**, 1852-1860.

**Zehmer, J. K., Bartz, R., Bisel, B., Liu, P., Seemann, J. and Anderson, R. G.** (2009). Targeting sequences of UBXD8 and AAM-B reveal that the ER has a direct role in the emergence and regression of lipid droplets. *J. Cell Sci.* **122**, 3694-3702.

**Zweytick, D., Leitner, E., Kohlwein, S. D., Yu, C., Rothblatt, J. and Daum, G.** (2000). Contribution of Are1p and Are2p to steryl ester synthesis in the yeast Saccharomyces cerevisiae. *Eur. J. Biochem.* **267**, 1075-1082.

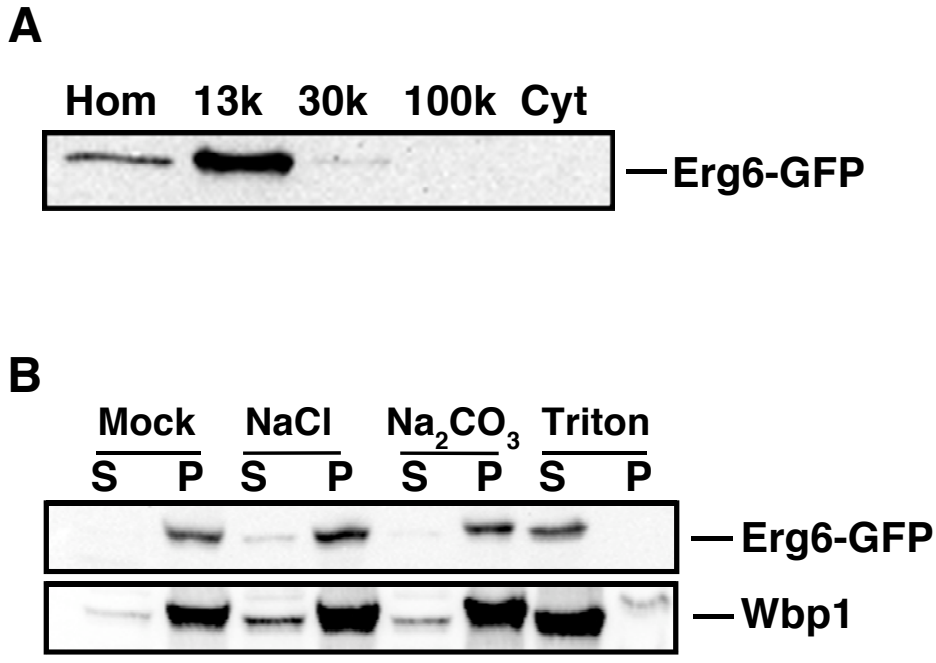
A
Hom
13k
30k
100k
Cyt
Erg6-GFP
B
Mock
NaCl
$Na_2CO_3$
Triton
S
P
S
P
S
P
S
P
Erg6-GFP
Wbp1

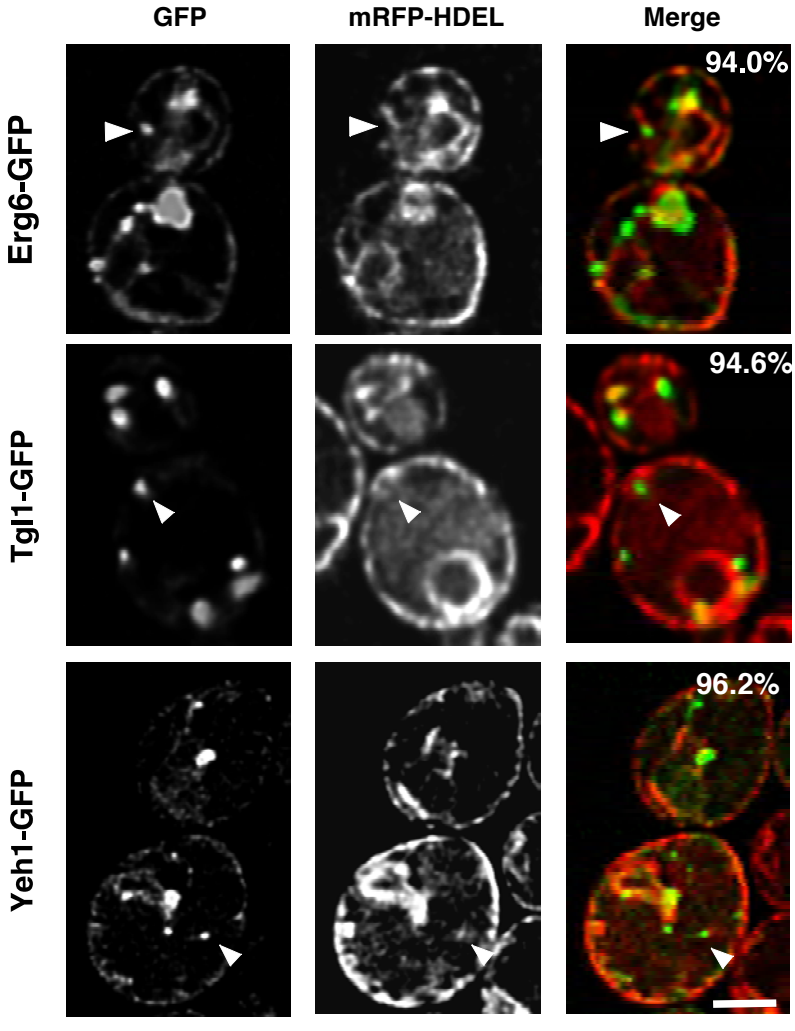
GFP
mRFP-HDEL
Merge
Erg6-GFP
Tgl1-GFP
Yeh1-GFP
94.0%
94.6%
96.2%

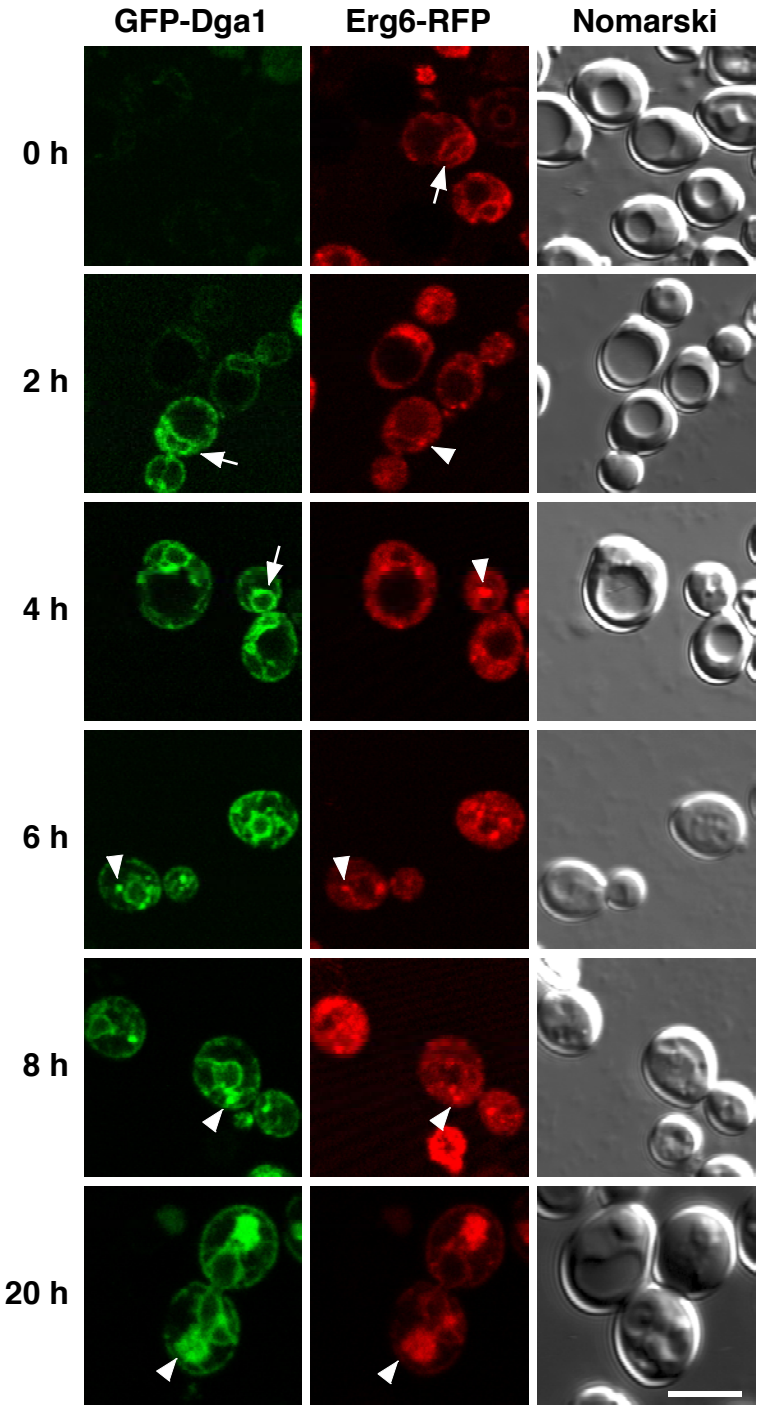
GFP-Dga1
Erg6-RFP
Nomarski
0 h
2 h
4 h
6 h
8 h
20 h

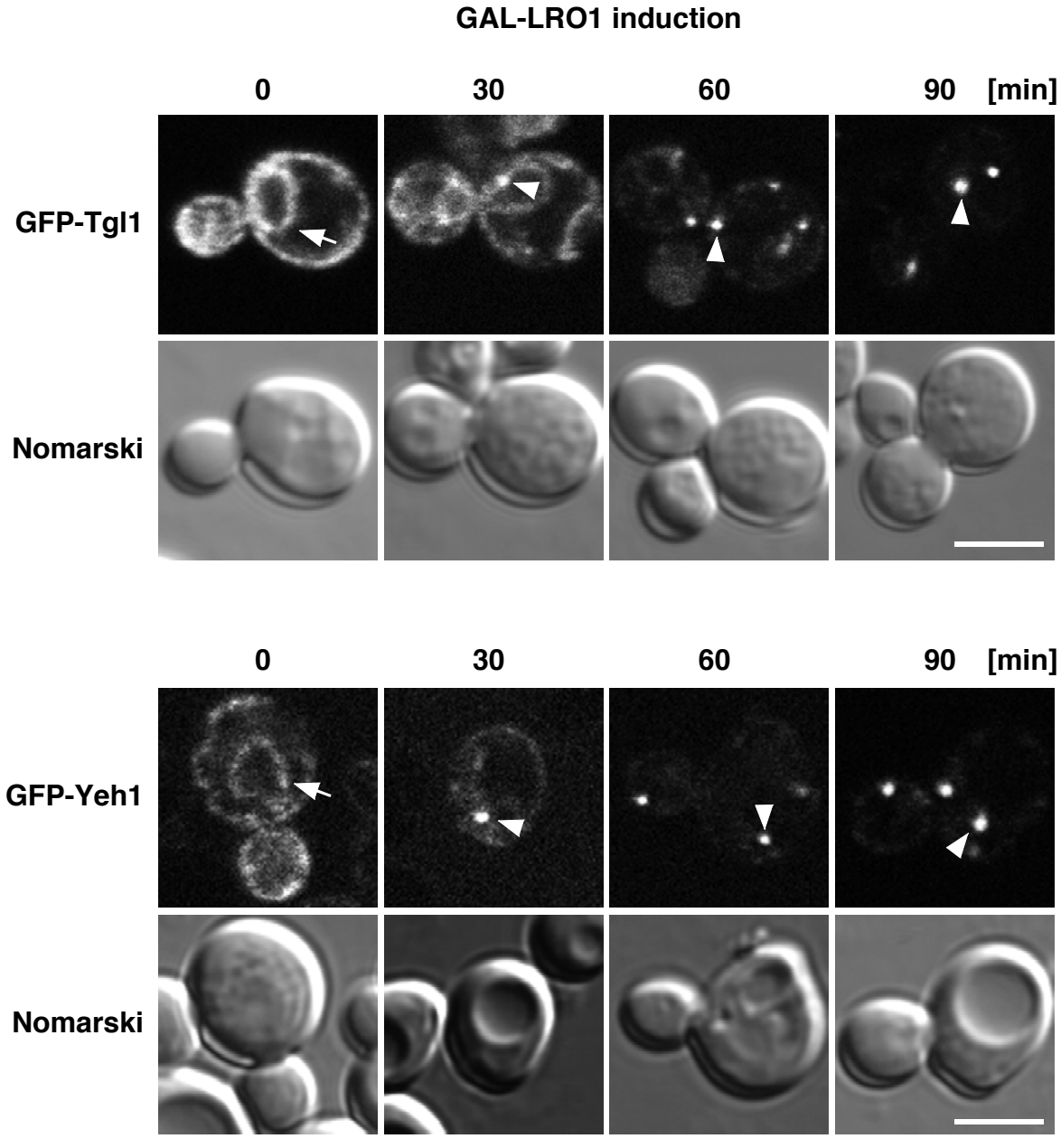
GAL-LRO1 induction
0
30
60
90
[min]
GFP-Tgl1
Nomarski
0
30
60
90
[min]
GFP-Yeh1
Nomarski

A

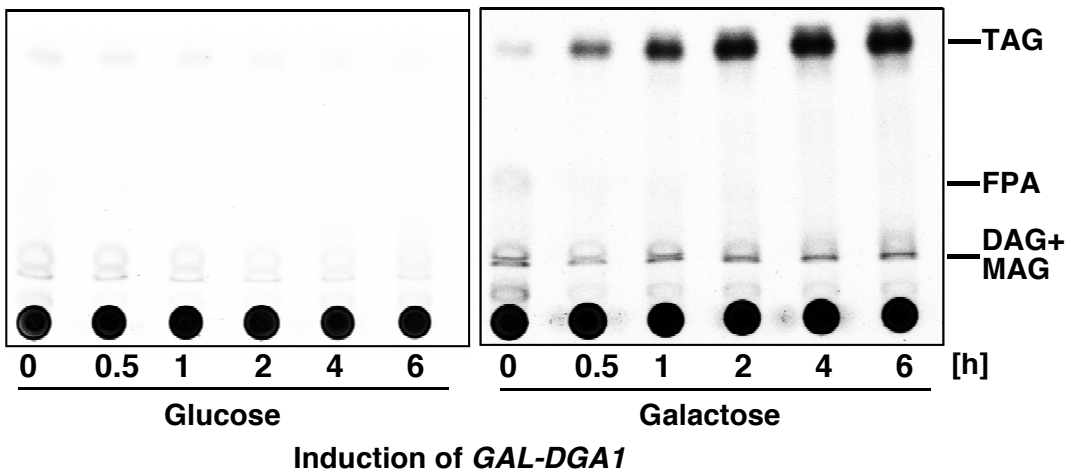
TAG
FPA
DAG+
MAG
0 0.5 1 2 4 6
0 0.5 1 2 4 6 [h]
Glucose
Galactose
Induction of GAL-DGA1

B

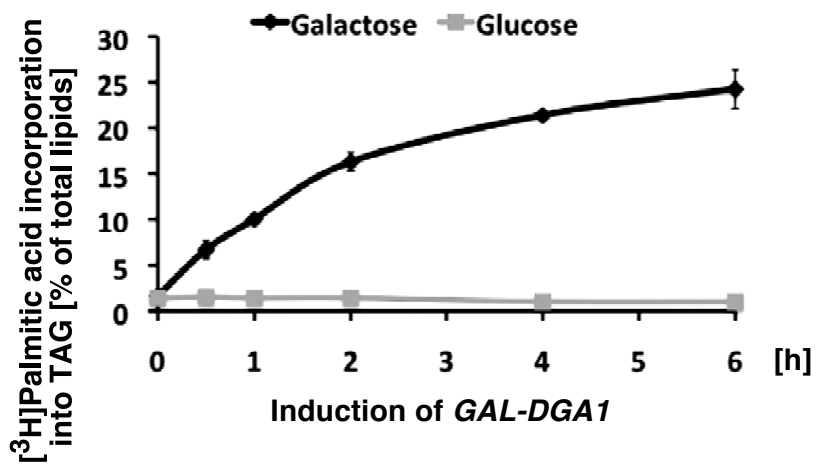
Galactose
Glucose
[3H]Palmitic acid incorporation into TAG [% of total lipids]
30
25
20
15
10
5
0
0 1 2 3 4 5 6 [h]
Induction of GAL-DGA1

C

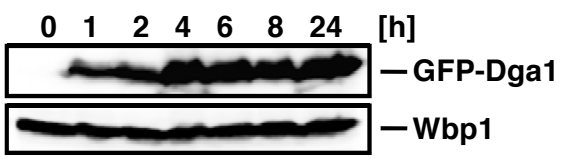
0 1 2 4 6 8 24 [h]
GFP-Dga1
Wbp1

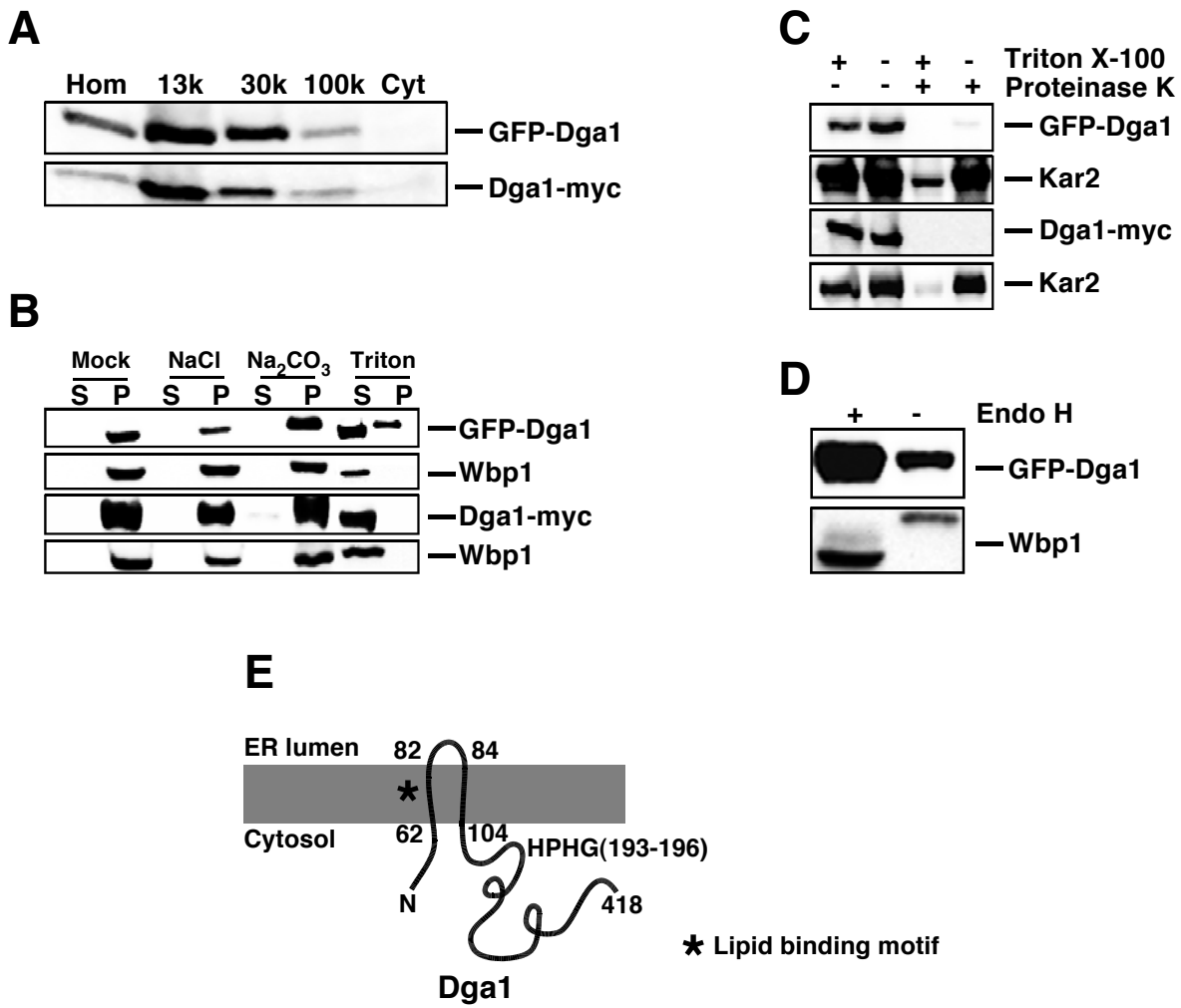
A
Hom
13k
30k
100k
Cyt
GFP-Dga1
Dga1-myc
B
Mock
NaCl
Na2CO3
Triton
S P S P S P S P
GFP-Dga1
Wbp1
Dga1-myc
Wbp1
C
+ - + - Triton X-100
- - + + Proteinase K
GFP-Dga1
Kar2
Dga1-myc
Kar2
D
+ - Endo H
GFP-Dga1
Wbp1
E
ER lumen
82
84
Cytosol
62
104
HPHG(193-196)
N
418
Lipid binding motif
Dga1

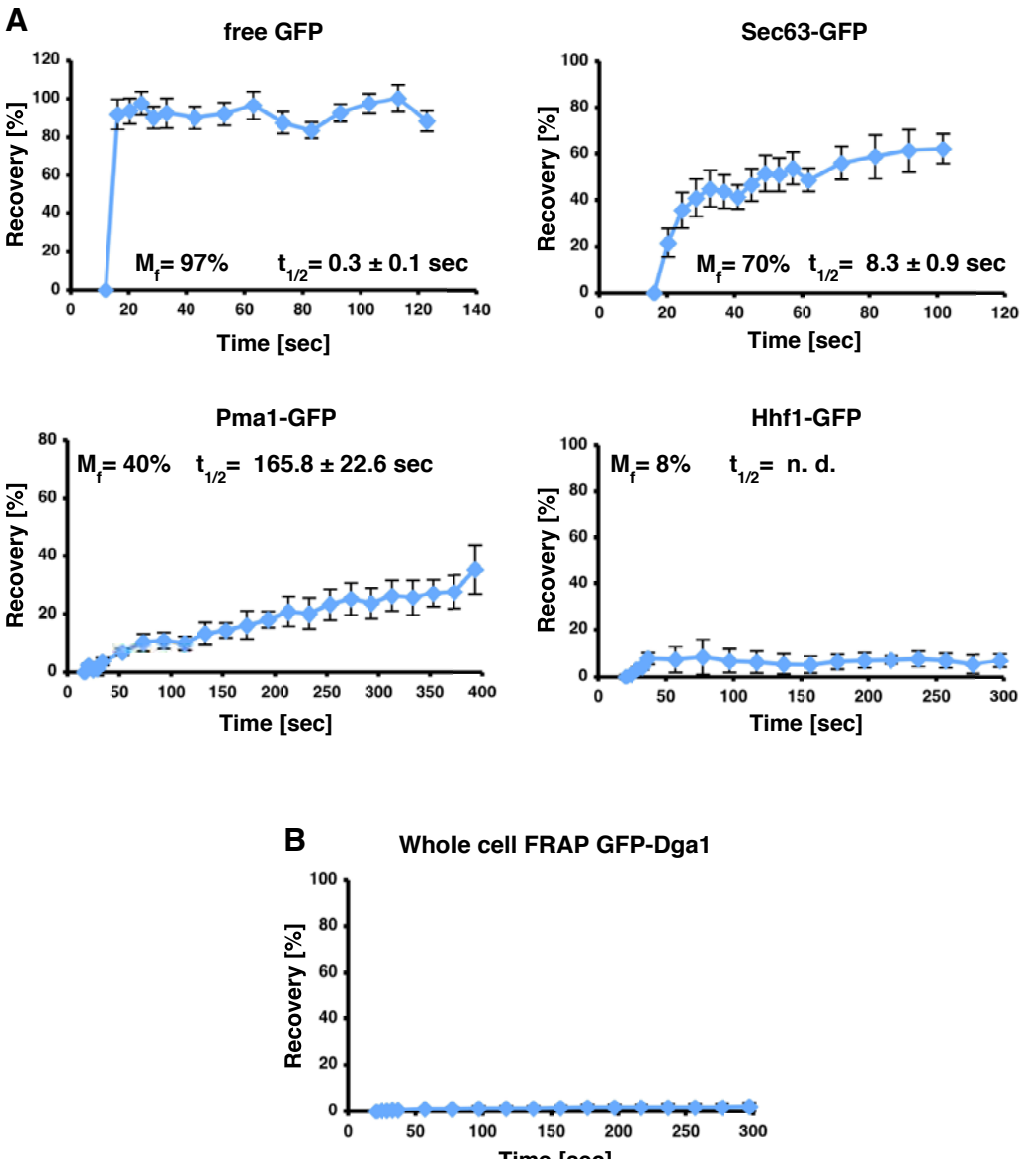
A
free GFP
Recovery [%]
Time [sec]
M_f = 97%
t_1/2 = 0.3 ± 0.1 sec
Sec63-GFP
M_f = 70%
t_1/2 = 8.3 ± 0.9 sec
Pma1-GFP
M_f = 40%
t_1/2 = 165.8 ± 22.6 sec
Hhf1-GFP
M_f = 8%
t_1/2 = n. d.
B
Whole cell FRAP GFP-Dga1

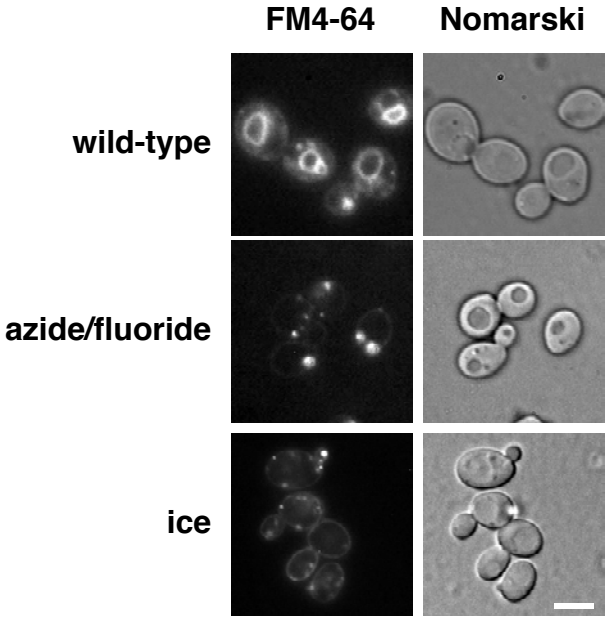
FM4-64
Nomarski
wild-type
azide/fluoride
ice

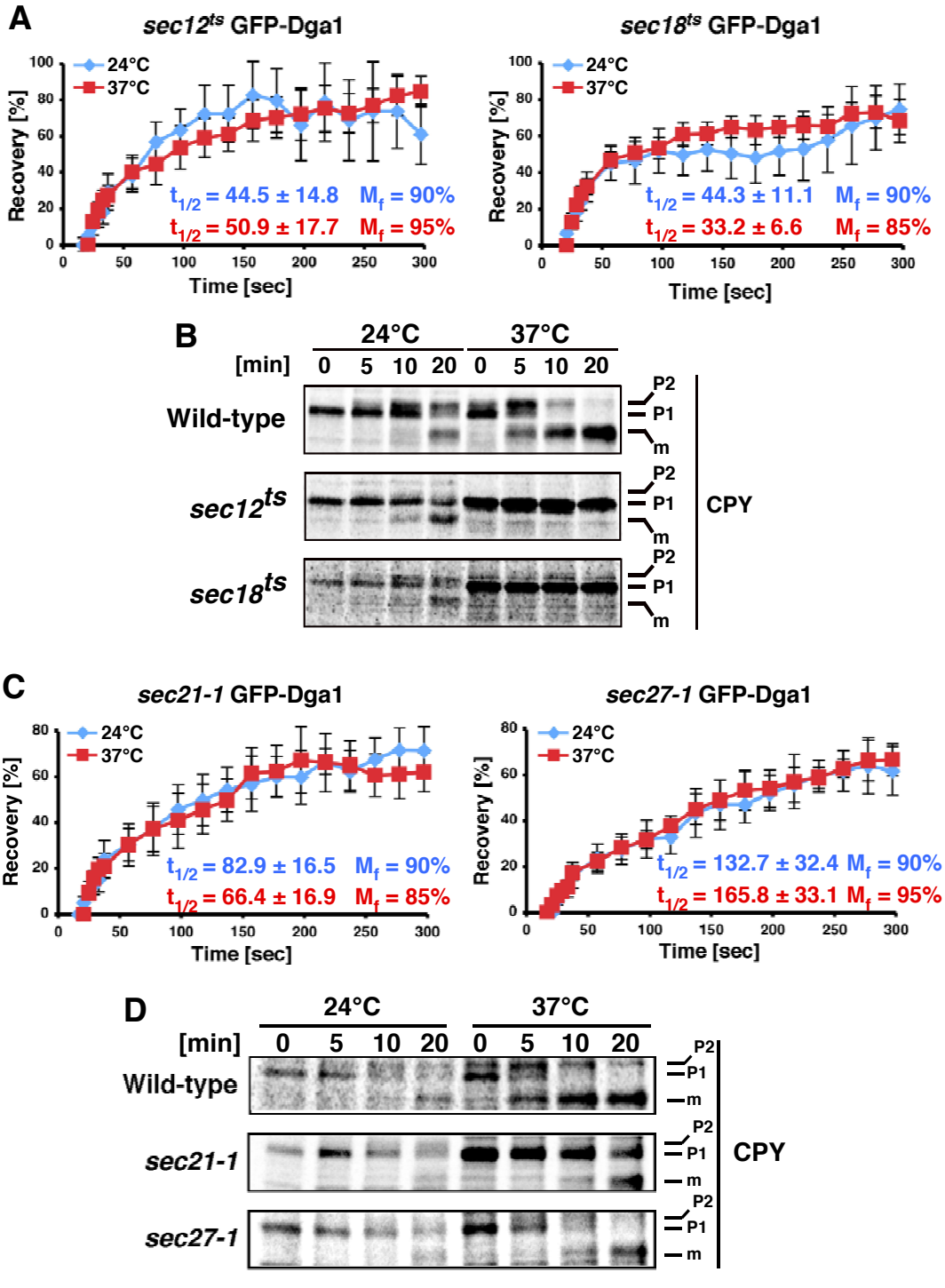
A
sec12ts GFP-Dga1
sec18ts GFP-Dga1
24°C
37°C
Recovery [%]
Time [sec]
t1/2 = 44.5 ± 14.8 Mf = 90%
t1/2 = 50.9 ± 17.7 Mf = 95%
t1/2 = 44.3 ± 11.1 Mf = 90%
t1/2 = 33.2 ± 6.6 Mf = 85%
B
24°C
37°C
[min]
0 5 10 20 0 5 10 20
Wild-type
sec12ts
sec18ts
P2
P1
m
CPY
C
sec21-1 GFP-Dga1
sec27-1 GFP-Dga1
t1/2 = 82.9 ± 16.5 Mf = 90%
t1/2 = 66.4 ± 16.9 Mf = 85%
t1/2 = 132.7 ± 32.4 Mf = 90%
t1/2 = 165.8 ± 33.1 Mf = 95%
D
sec21-1
sec27-1

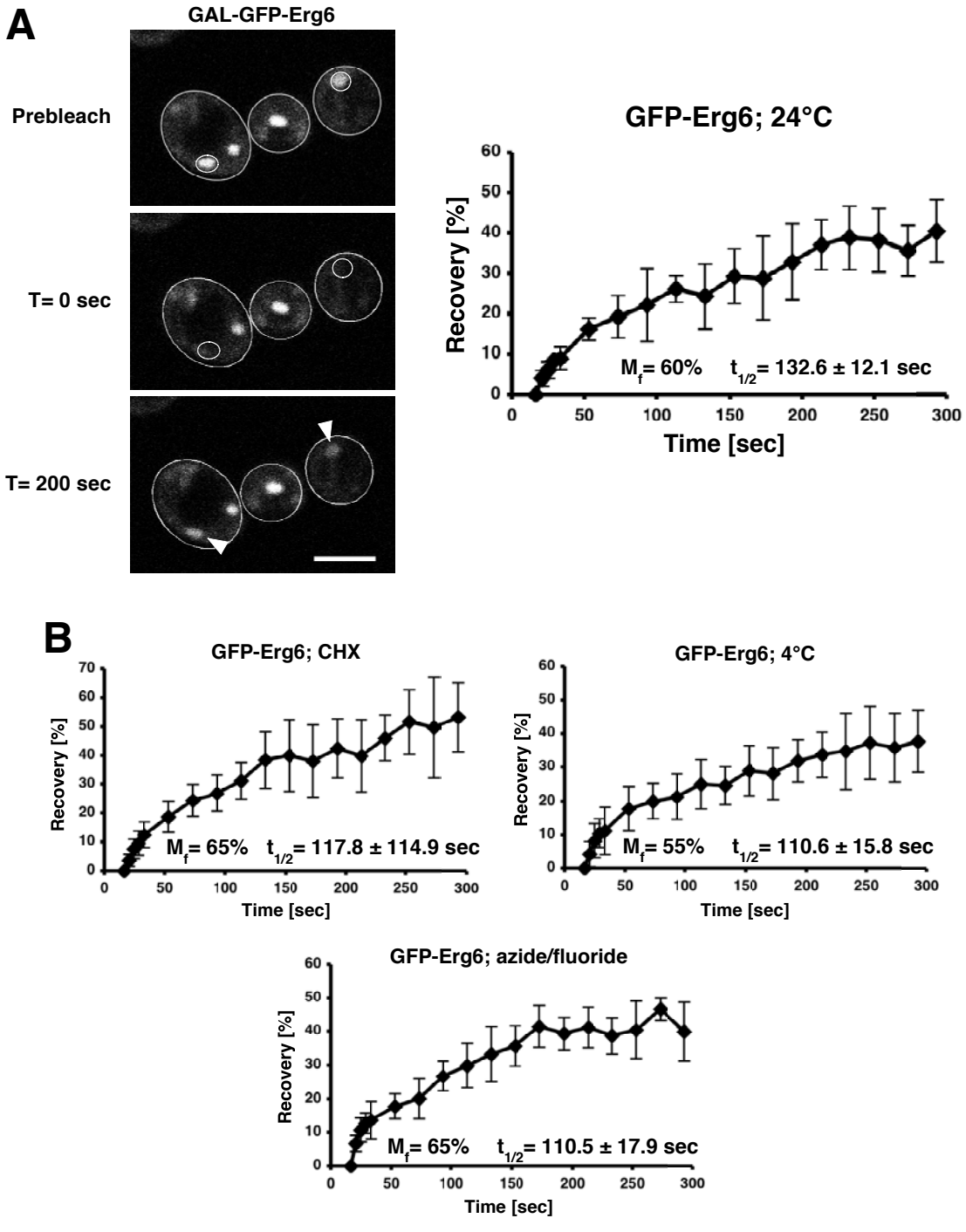
A
GAL-GFP-Erg6
Prebleach
T= 0 sec
T= 200 sec
GFP-Erg6; 24°C
Recovery [%]
Time [sec]
M_f= 60%
t_1/2= 132.6 ± 12.1 sec
B
GFP-Erg6; CHX
M_f= 65%
t_1/2= 117.8 ± 114.9 sec
GFP-Erg6; 4°C
M_f= 55%
t_1/2= 110.6 ± 15.8 sec
GFP-Erg6; azide/fluoride
M_f= 65%
t_1/2= 110.5 ± 17.9 sec

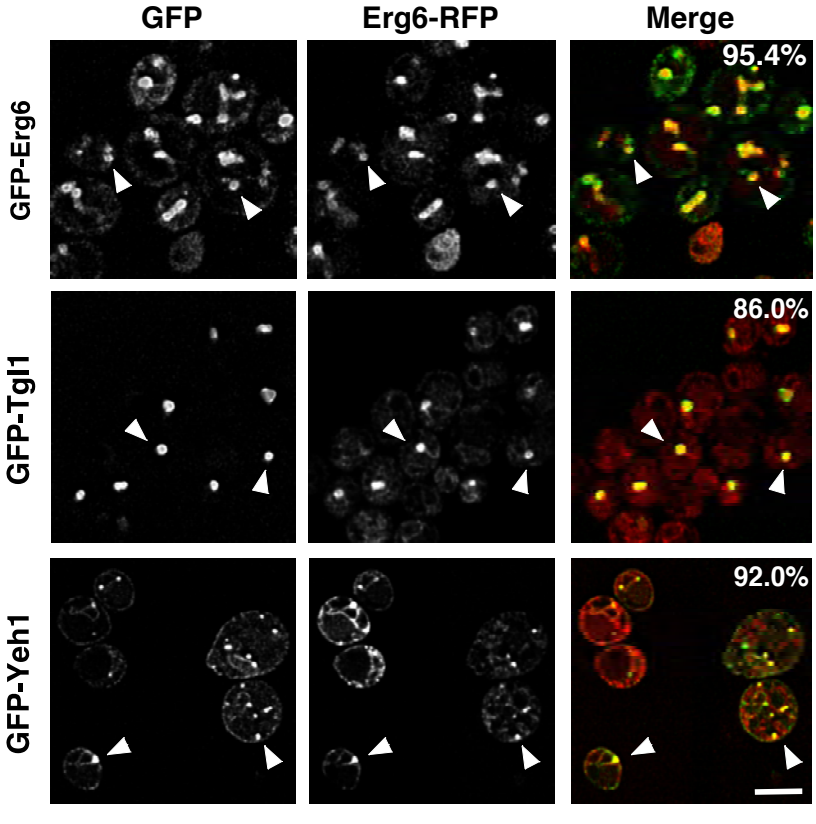
GFP
Erg6-RFP
Merge
GFP-Erg6
GFP-Tgl1
GFP-Yeh1
95.4%
86.0%
92.0%

**Table S1.** *S. cerevisiae* strains used in this study

| Strain | Relevant Genotype | Source |
|---|---|---|
| RSY1533 | *MATα leu2Δ0 ura3Δ0 his3Δ1 lys2Δ0 MET15* | Euroscarf |
| RSY2307 | *MATα leu2Δ0 ura3Δ0 his3Δ1 lys2Δ0 pGAL-PMA1-GFP-URA3* | This Study |
| RSY3000 | *MATα dga1::URA3 lro1::TRP1 are1::HIS3 are2::LEU2 ADE2 HDEL-RFP-URA3 ERG6-GFP::KanMX* | This Study |
| RSY3021 | *MATα his3Δ1 leu2Δ0 lys2Δ0 ura3Δ0 are1::KanMX are2::KanMX trp1::URA3 GAL-LRO1::TRP1 dga1::loxP* | This Study |
| RSY3097 | *MATα his3Δ1 leu2Δ0 lys2Δ0 ura3Δ0 are1::KanMX are2::KanMX ERG6-GFP::HIS3* | This Study |
| RSY3272 | *MATα his3Δ1 leu2Δ0 lys2Δ0 ura3Δ0 ERG6-GFP::HIS3* | This Study |
| RSY3292 | *MATα his3Δ1 leu2Δ0 lys2Δ0 ura3Δ0 are1::KanMX are2::KanMX trp1::URA3 lro1::loxP GAL-GFP-DGA1::HIS3* | This Study |
| RSY3337 | *MATα his3Δ1 leu2Δ0 lys2Δ0 ura3Δ0 are1::KanMX are2::KanMX trp1Δ lro1::loxP GAL-GFP-DGA1::HIS3 pURA3-GAL-ERG6-RFP* | This Study |
| RSY3402 | *MATα his3Δ1 leu2Δ0 lys2Δ0 ura3Δ0 pURA3-GAL-GFP-ERG6* | This Study |
| RSY3482 | *MATα his3Δ1 leu2Δ0 lys2Δ0 ura3Δ0 are1::KanMX are2::KanMX lro1::loxP DGA1-myc::HIS3* | This Study |
| RSY3604 | *MATα his3Δ1 leu2Δ0 lys2Δ0 ura3Δ0 are1::KanMX are2::KanMX trp1::URA3 lro1Δ::TRP1 dga1::loxP pLEU2-GAL-GFP-TGL1 pURA3-HDEL-RFP* | This Study |
| RSY3605 | *MATα his3Δ1 leu2Δ0 lys2Δ0 ura3Δ0 are1::KanMX are2::KanMX trp1::URA3 lro1Δ::TRP1 dga1::loxP pLEU2-GAL-GFP-YEH1 pURA3-HDEL-RFP* | This Study |
| RSY3755 | *MATα his3Δ1 leu2Δ0 lys2Δ0 ura3Δ0 are1::KanMX are2::KanMX lro1::loxP HIS3-GAL-DGA1* | This Study |
| RSY3758 | *MATα his3Δ1 leu2Δ0 lys2Δ0 ura3Δ0 dga1::KanMX lro1::KanMX ERG6-GFP::HIS3* | This Study |
| RSY3770 | *MATα his3Δ1 leu2Δ0 lys2Δ0 ura3Δ0 trp1Δ are1::KanMX are2::KanMX GAL-LRO1::TRP1 dga1::loxP pERG6-RFP-URA3* | This Study |
| RSY4359 | *MATα his3Δ1 leu2Δ0 lys2Δ0 ura3Δ0 pGAL-GFP-DGA1-URA3* | This Study |
| RSY4399 | *MATα his3Δ1 leu2Δ0 lys2Δ0 ura3Δ0 pGAL-GFP-URA3* | This Study |
| RSY4452 | *MATα his3Δ1 leu2Δ0 lys2Δ0 ura3Δ0 pSEC63-GFP-URA3* | This Study |
| RSY4461 | *MATa sec12$^{ts}$ ade2 his3 ura3 can1 pGAL-GFP-DGA1-URA3* | This Study |
| RSY4465 | *MATα sec18$^{ts}$ his3Δ1 leu2Δ0 LYS2 ura3Δ0 pGAL-GFP-DGA1-URA3* | This Study |
| RSY4509 | *MATα his3Δ1 leu2Δ0 lys2Δ0 ura3Δ0 pGAL-GFP-DGA1-* | This Study |

| | | |
|---|---|---|
| | *URA3 pERG6-RFP-LEU2* | |
| RSY4534 | *MATα his3Δ1 leu2Δ0 lys2Δ0 ura3Δ0 trp1Δ are1::KanMX are2::KanMX GAL-LRO1::TRP1 dga1::loxP pADH-GFP-TGL1-HIS3* | This Study |
| RSY4535 | *MATα his3Δ1 leu2Δ0 lys2Δ0 ura3Δ0 trp1Δ are1::KanMX are2::KanMX GAL-LRO1::TRP1 dga1::loxP pADH-GFP-YEH1-HIS3* | This Study |
| RSY4612 | *MATα leu2Δ0 ura3Δ0 his3Δ1 lys2Δ0 fld1::KanMX pGAL-GFP-DGA1-URA3* | This Study |
| RSY4695 | *MATα his3Δ1 leu2Δ0 lys2Δ0 ura3Δ0 are1::KanMX are2::KanMX trp1Δ lro1::loxP fld1::loxP GAL-GFP-DGA1::HIS3 pURA3-GAL-ERG6-RFP* | This Study |
| RSY4757 | *MAT? sec21-1 his3Δ1 leu2Δ0 ura3Δ0 pGAL-GFP-DGA1-URA3* | This Study |
| RSY4758 | *MAT? sec27-1 his3Δ1 leu2Δ0 ura3Δ0 pGAL-GFP-DGA1-URA3* | This Study |
| RSY4842 | *MATa his3Δ1 leu2Δ0 met15Δ0 ura3Δ0 HHF1-GFP-HIS3* | This Study |